

**Aligning Acute and Chronic Functional Readouts and Utilizing Zolpidem to Improve
Neurological Impairments After Cardiac Arrest**

by

David Fine

B.S. Biochemistry, University of Vermont, 2012

Submitted to the Graduate Faculty of the
Dietrich School of Arts and Sciences in partial fulfillment
of the requirements for the degree of
Master of Science

University of Pittsburgh

2020

UNIVERSITY OF PITTSBURGH

DIETRICH SCHOOL OF ARTS AND SCIENCES

This thesis was presented

by

David Fine

It was defended on

June 22, 2020

and approved by

Dr. Ed Dixon, Ph.D, Department of Neurosurgery, Department of Neuroscience

Dr. Amy Wagner, MD, Department of Physical Medicine and Rehabilitation, Department of Neuroscience

Dr. Steven Meriney, Ph.D, Department of Neuroscience

Thesis Advisor/Dissertation Director: Dr. Amy Wagner, MD, Department of Physical Medicine and Rehabilitation, Department of Neuroscience

Copyright © by David Fine

2020

Aligning Acute and Chronic Functional Readouts and Utilizing Zolpidem to Improve Neurological Impairments After Cardiac Arrest

David Fine, MS

University of Pittsburgh, 2020

While cardiac arrest survival rates have improved alongside recent advances in modern resuscitation techniques and targeted temperature management, many survivors experience multiple ongoing symptoms after their hypoxic-ischemic brain injury (HIBI) including movement disorders, depression, and low cognitive arousal. Neurological assessments like the neurological deficit score (NDS), and physiological readouts from blood chemistry values are used to assess acute post-injury outcome, but little has been done to evaluate how these acute readouts distinguish heterogeneity within the injury population, or how they align with long term behavioral and neurological outcomes as a prognostic tool. Recent evidence also highlights zolpidem as an effective treatment for post-HIBI symptoms, but its clinical use has been met with mixed results. This study utilized a regression model and correlational analyses to evaluate associations among NDS, blood lactate, and blood acid base excess values as acute post-injury readouts, behavioral outcome, and dopamine neurotransmission outcomes obtained via fast scan cyclic voltammetry two weeks after a 5-min asphyxia cardiac arrest (ACA). A pilot study was also performed to evaluate the effects of chronic systemic zolpidem administration on improving behavioral outcomes and reversing striatal hyper-dopaminergia after ACA. NDS significantly aligned with survival probability after ACA. NDS and both blood chemistry readouts aligned with several behavioral and dopamine neurotransmission outcomes, and several dopaminergic and behavioral outcomes robustly correlated with one another. Additionally, chronic zolpidem reflexive and

cognitive behavioral outcomes, as defined by the acoustic startle response and the sucrose preference test, respectively. This work highlights novel associations between post-HIBI behavioral and neurological outcomes as well as benefits of chronic zolpidem administration in ameliorating post-HIBI neurological sequelae. Future work should further characterize the effects of zolpidem administration after cardiac arrest and utilize molecular assays to identify protein expression changes that will unravel neurobiological mechanisms driving HIBI-induced functional impairments and highlight therapeutic targets to treat CA survivors.

Table of Contents

Preface.....	x
1.0 Introduction.....	1
2.0 Methods.....	11
3.0 Results	21
4.0 Regional Zolpidem Microinjections To Reverse HIBI-Induced Striatal Hyperdopaminergia – A Conceptual Experiment	39
5.0 Discussion.....	50
6.0 Conclusion	64
Bibliography	66

List of Tables

Table 1: Equations and parameters utilized in stimulations.	17
Table 2: Cox regression model of study exclusion (due to death/distress) on standardized NDS, lactate, and ABE median scores (n=45, number of events=25).	26
Table 3: Median probabilities of ACA animals surviving to D3, D6, and D7 post-injury... ..	26
Table 4: Spearman’s rank correlations show associations between median NDS and D14 NDS, median lactate, and median ABE values.....	27
Table 5: Spearman’s rank correlations show associations between injury metrics and DA release-based metrics.	28
Table 6: Spearman’s rank correlations show associations between injury metrics and DA reuptake-based metrics.	28
Table 7: Spearman’s rank correlations show associations between injury metrics and behavioral outcomes.	29
Table 8: Summary of association pairs from partial correlation analyses (Spearman’s rank correlations) which significantly changed after adjusting for ABE.....	30
Table 9: Injury and treatment group counts.....	43

List of Figures

Figure 1: Graphical depiction of neurotransmitter pathways feeding involved in polysynaptic intrastriatal circuitry that support coordinated movement and also arousal and consciousness (Davis/Wagner 2019)..... 4

Figure 2: Uninjured striatal-pallidal-nigral circuit (A) and HIBI-affected striatal-pallidal-nigral circuit (B)..... 6

Figure 3: Schematic representation of acoustic startle response circuit. 7

Figure 4: Mechanistic theory of HIBI-affected striatal-pallidal-nigral circuitry before (A) and after (B) systemic zolpidem administration. 9

Figure 5: Schematic outlining FSCV experimental design and median forebrain bundle stimulation sequence..... 15

Figure 6: Scatterplots show blood lactate values for ACA (a) and Sham (b) groups at baseline, D1-D3 (median), D7 and D14 post-surgery..... 21

Figure 7: Scatterplots show blood lactate values for ACA (a) and Sham (b) groups at baseline, D1-D3 (median), D7 and D14 post-surgery..... 22

Figure 8: Scatterplots show blood acid-base excess (ABE) values for ACA (a) and Sham (b) groups at baseline, D1-D3 (median), D7 and D14 post-surgery. 23

Figure 9: Median values for NDS at D1 – D3 post-injury, represented by bars, show acute neurological outcome after 5min ACA. 24

Figure 10: Scatterplots of NDS (a), lactate (b), and ABE (c) values show differences between survivors and non-survivors after ACA injury..... 25

Figure 11: Mean \pm SEM for acoustic startle responses at 85 dB (8a, 8d), 95 dB (8b, 8e), and 105 dB (8c, 8f) sound bursts shown as a percent change from baseline to 3 days post-surgery. 31

Figure 12: Mean \pm SEM values for myoclonic responses observed D2 following ACA/sham surgery. 32

Figure 13: Mean \pm SEM values for distance traveled in the OFT D7 post-surgery. 33

Figure 14: Mean \pm SEM values for exploratory zone entries in the open field D7 post-surgery. 34

Figure 15: Mean \pm SEM of sucrose preference calculated on D8 post-surgery. 35

Figure 16: Mean \pm SEM of maximal evoked DA overflow (a) and evoked DA overflow 1s into stimulation (b) in the D-STR following 60Hz, 10s MFB stimulations two weeks post-surgery. 36

Figure 17: Mean \pm SEM values of total DA released (a) and initial DA release rate (b) in the D-STR following 60Hz,10s stimulation two weeks post-surgery. 37

Figure 18: Mean \pm SEM maximal DA reuptake velocity (V_{max}) (a) and K_{mi} (b) for each group. 38

Figure 19: Schematic representation of FSCV experimental study and microinjection timepoints. 44

Figure 20: Proposed effects of intra-pallidal zolpidem 47

Figure 21: Schematic of acoustic startle response pathway influenced by HIBI. 56

Figure 22: Effects of HIBI on basal ganglia circuitry before (A) and after (B) systemic donepezil administration. 62

Preface

I would like to thank Dr. Ed Dixon and Dr. Steven Meriney for acting as my thesis committee, and Dr. Amy Wagner for all the support and guidance she has provided as my thesis advisor and acting committee member. Thank you to Dr. Tomas Drabek, Dr. Rehana Leak, and Dr. Patrick Kochanek for providing endless guidance and support as part of our “cardiac arrest research team”. Special thanks to Jason Stezoski for performing our experimental CA surgeries. I would also like to thank Nabil Awan for providing expertise and guidance in statistical analyses, as well as Aaron Braverman, Dr. William (Austin) Davis, and Tyler Shick for their assistance with literature reviews, data analyses, and graphics generation throughout this process.

I could not have done this without you all! Thanks again.

1.0 Introduction

The annual incidence of out-of-hospital cardiac arrest (CA) in the U.S. is approximately 360,000 cases per year¹. While CA survival rates have improved alongside recent advances in modern resuscitation techniques and targeted temperature management, prevalence of good functional outcomes after neurorehabilitation is as low as 6%^{2,3}, leaving many individuals with multiple ongoing symptoms. In addition to disorders of consciousness (DoC), anxiety/depression, agitation/restlessness, and low cognitive arousal, the hypoxic-ischemic brain injury (HIBI) resulting from CA afflicts survivors with a variety of movement disorders ranging from abnormal, involuntary movements and seizure to more parkinsonian symptoms like dystonia, chorea, and tremor⁴. Though these symptoms overlap with other neurological disorders, many of which involve striatal dopamine (DA) dysfunction, CA survivors represent a “new” clinical population, and little work has been done to develop effective treatments to combat CA pathology.

CA survivors share many cognitive features with individuals who have suffered a significant traumatic brain injury (TBI), and current clinical practice for HIBI treatment borrows approaches used with other brain injury populations. However, the pathologies underlying HIBI and TBI symptoms may differ greatly depending on injury etiology. Experimental TBI studies suggest a state of striatal *hypodopaminergia* or suppressed DA neurotransmission following the injury, prompting the use of DA agonists like methylphenidate to improve symptoms accompanying the injury⁵. Using a rodent model of ventricular fibrillation cardiac arrest (VF-CA) paired with fast scan cyclic voltammetry (FSCV) to conduct *in vivo*, real time characterization of presynaptic DA, our research team discovered abnormally elevated DA neurotransmission two weeks following the injury, which is worsened by methylphenidate administration⁶.

The cause of CA also influences both the duration of ischemia and the cerebral blood flow changes during brain reperfusion, two key factors that determine the injury outcome⁷. Asphyxia cardiac arrest (ACA) arises from respiratory failure, as seen with intoxication, drowning, or trauma, and causes more severe morphologic brain damage than VF-CA⁸. ACA also exhibits different brain reperfusion characteristics than VF-CA which affect more brain regions – ACA-induced hyper-perfusion of both the cortex and thalamus whereas VF-CA only leads to early hyperperfusion of the cortex⁷.

Additionally, ACA is a dynamic injury impacted by many variables in clinical settings and in experimental models. For example, the ischemic brain is sensitive to temperature such that small differences in ambient temperature critically influence neuropathological outcomes in brain regions responsible for motor behavior and cognition^{9,10}. Insult severity also varies within the same injury model and even within the same breed of rat (Sprague-Dawley) across multiple vendors¹¹.

Neurological assessments are often used to assess acute post-injury outcome. Neurological deficit scores (NDS) have been utilized to evaluate the effects of hypothermia¹², as well as the differential effects of sodium bicarbonate and epinephrine dosages on initial recovery¹³ from CA which has aided resuscitation management advancements. Physiological assessments such as blood chemistry readings are also utilized to assess post-injury outcome. Blood lactate levels, for example, strongly correlate with mortality after CA which contribute to early patient prognosis¹⁴. However, research exploring associations between physiological readouts and functional outcomes is lacking in several areas. For example, most studies focus on acute timepoints rather than more long-term outcomes. With regard to experimental ischemic injury models, little work has been done in utilizing these readouts to 1) identify heterogeneity within individual injury

models, and 2) evaluate how these readouts align with, and influence behavioral outcomes. HIBI symptomologies implicate striatal DA dysfunction and elevated striatal DA levels have been reported following VF-CA⁶ and ACA, the latter of which has been shown to induce deficits in reflexive, exploratory, and cognitive behavior (Not yet published). As such, exploring associations between acute physiological readouts and DA neurotransmission outcomes may offer mechanistic insight to post-HIBI neurological sequelae and highlight potential therapeutic targets.

HIBI affects certain brain regions more than others, with damage localized to the brain's vascular watershed and metabolically demanding neuronal subtypes within the hippocampus, thalamus, cerebellum, and cortex^{15,16}. Striatal medium spiny neurons (MSNs) are also particularly vulnerable to ischemic damage^{17,18} and exhibit early, irreversible damage from ischemia¹⁹. These GABAergic neurons make up 80-90% of the striatal population and receive dense DAergic input from the substantia nigra pars compacta (SNpc). Also, through their modulation of cortical glutamatergic input and aspiny acetylcholine (ACh) interneurons, MSNs play key roles in cognition, behavior, motivation, and controlled movement. MSNs receive MSNs with type 2 DA receptors (D2Rs), which are associated with dystonia, chorea, and cognitive disorders²⁰⁻²⁴ are particularly vulnerable to Huntington's Disease-like metabolic dysfunction/damage^{25,26}. Evidence also shows uncontrolled striatal DA release seen after even a mild hypoxic-ischemic insult which is more severe than ischemia-induced increases of other neurotransmitters^{27,28}. As aberrant DA signaling underlies movement disorders in Parkinson's disease (PD) and HD²⁹, DA neurotransmission changes after CA may facilitate HIBI-induced motor abnormalities. The thalamic reticular nucleus (tRN) is also particularly vulnerable to ischemic injury. Another primarily GABAergic region, the tRN provides inhibitory modulation of the intralaminar (iLN) thalamus, a crucial component of the reticular activating system (RAS) which, through its

communication with the cortex, regulates conscious states. HIBI-induced neuronal damage in the tRN likely facilitates abnormal thalamocortical signaling that drives DoC after CA.

Further, disinhibited DA release and imbalance of other DA neurotransmission elements like ACh may also lead to cognitive disorders that impair function after CA^{30–32}. Figure 1 depicts the relevant neurotransmitter pathways involved in striatal circuitry that support coordinated movement, arousal, and consciousness as well as the consequences of HIBI on their functionality.

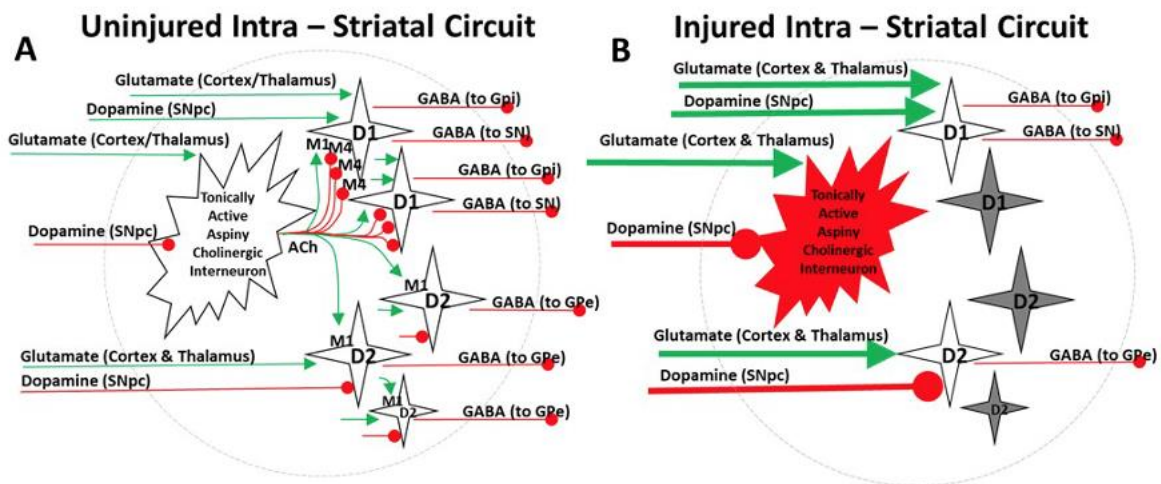


Figure 1: Graphical depiction of neurotransmitter pathways feeding involved in polysynaptic intrastriatal circuitry that support coordinated movement and also arousal and consciousness (Davis/Wagner 2019).

(A) Uninjured Circuit: DAergic projections from the SNpc provide excitatory input into D1 MSNs and inhibitory input into D2 MSNs. DAergic stimulation of MSNs is modulated by cholinergic input from aspiny neurons and from glutamatergic cortico-striatal afferents. M4 activation on D1 MSNs blunt MSN output while M1 activation on both D1 and D2 MSNs provides an excitatory effect; generalized muscarinic stimulation leads to D1 MSN inhibition, and D2 MSN activation modulates the impacts of DA and glutamate on GABAergic MSN pallidal-thalamic relays and nigral projections. (B) Injured Circuit: HIBI results in damage/loss of metabolically vulnerable MSNs. Reduced GABAergic pallidal outflow by HIBI reduces GPI inhibitory output to thalamus, facilitates excitotoxicity from subthalamic nucleus projections, causes delayed damage to GABAergic neurons in SNpr that may facilitate hyperdopaminergia observed in our ACA model.

Elevated DA levels post-HIBI may excessively inhibit tonically active spiny Ach neurons that then promotes overactivation of remaining D1 MSNs and overinhibition of remaining D2 MSNs.

Legend: MSN, Medium Spiny Neuron; HIBI, hypoxic ischemic brain injury; SNpr, Substantia nigra pars reticulata; DA, Dopamine; Ach, acetylcholine. (Green—excitatory effects on post-synaptic neuronal firing, red—inhibitory on post-synaptic neuronal firing. Bolded colors represent augmented neurotransmission effects due to HIBI. Grey—dying/dysfunctional MSNs.

Striatal MSNs project topographically to the internal and external globus pallidus (GPi and GPe, respectively) as part of the “direct” and “indirect” pathways of movement, as well as to the substantia nigra pars reticulata (SNpr) and SNpc. Striatal DA release by dopaminergic SNpc projections are regulated in part by direct and indirect GABAergic feedback from MSNs^{33–35} and this GABAergic control of the SNpc strongly influences its firing properties³⁴. GABAergic afferents from the GPe also strongly influence the firing properties of both nigral regions^{34,36,37}. MSNs and GABAergic interneurons also provide inhibitory feedback to spiny ACh interneurons and with each other, creating complex intra-striatal networks and functional units that influence the larger striatal-pallidal-thalamic circuitry underlying coordinated movement and consciousness. Given these ideas, disrupted GABAergic outflow resulting from MSN damage and dysfunction may facilitate striatal hyperdopaminergia and abnormal thalamocortical transmission that manifests itself as movement and hypoarousal disorders. Given the specific vulnerability of striatal MSNs to ischemia, this evidence suggests that altering GP-mediated GABAergic feedback to the SNpc may reverse striatal hyperdopaminergia after HIBI and ameliorate movement disorders and DoC.

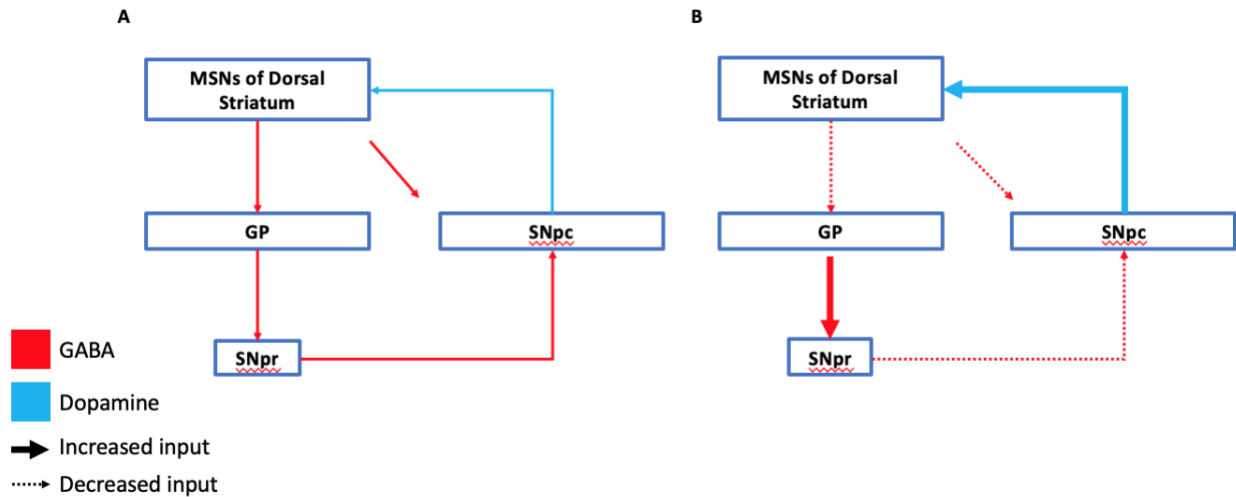


Figure 2: Uninjured striatal-pallidal-nigral circuit (A) and HIBI-affected striatal-pallidal-nigral circuit (B). (B) Hypoxic ischemic brain injury (HIBI) leads to acute striatal neuron dysfunction with selective D2 MSN vulnerability. The resulting increase in pallidal (GP) outflow inhibits GABAergic SNpr neurons and indirectly dis-inhibiting SNpc DAergic neurons, thus leading to elevated striatal DA levels.

Depression is a major symptom observed after both traumatic and ischemic brain injury, with roughly 40% of stroke patients suffering from post-stroke depression (PDS)38,39. Though anhedonia, the reduced ability to experience pleasure, is relatively easy to identify using animal models, its neurobiological underpinnings are not well understood. As dopaminergic signaling plays a key role in pleasurable experiences, with mesolimbic dopaminergic neurons encoding the information eliciting motivational value and motivational salience40-42, normalizing HIBI-induced DA neurotransmission aberrations may ameliorate depression symptoms following ACA. Inflammation likely influences post-HIBI behavioral abnormalities as well. The inflammatory response to systemic infections influences central nervous system changes that facilitate symptoms referred to as sickness behaviors. Through its effects on DA signaling, inflammation has been shown to affect basal ganglia-relevant behaviors such as motivation and motor activity43-45. Elevated microglial activation and striatal tumor necrosis factor alpha (TNF α) after VF-CA46

suggest that ongoing neuroinflammation may also contribute to post-HIBI behavioral abnormalities.

The acoustic startle response (ASR) also plays an important role in neuropsychiatric disease studies because its disruption often indicates broader neurological problems. It demonstrates a phenomenon called pre-pulse inhibition (PPI), a type of stimulus desensitization affected in several neurological disorders associated with DA signaling abnormalities. TBI, which is shown to suppress DA neurotransmission, induces a long-lasting suppression of the ASR as well⁴⁷. Schizophrenia and HD, disorders associated with hyperactive DA, provoke an amplified ASR as well as PPI deficits^{48–50}. The ASR is mediated by a tri-synaptic pathway in the lower brainstem and spinal cord and is depicted in Figure 3. Auditory information is translated into neural signals at the cochlear nuclei. The cochlear nuclei then relay these signals via the 8th cranial nerve to the pontine reticular nucleus (PnC) whose projections innervate hundreds of motor neurons, via the reticulospinal tract in the medial longitudinal fasciculus of the spinal cord, in response to the stimulus^{51,52}.

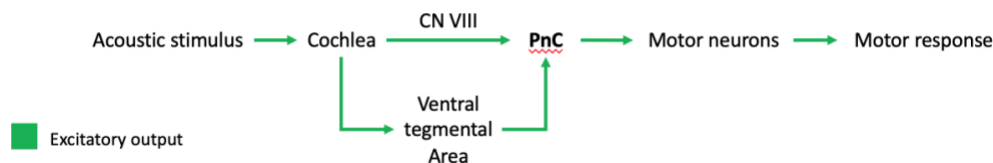


Figure 3: Schematic representation of acoustic startle response circuit.

The pontine reticular formation (pRF), particularly its caudal nucleus, The pRF acts as a sensorimotor interface where the transition of sensory input into motor output can be directly influenced by excitatory or inhibitory afferents, thus playing an important role in mediating the ASR⁵³.

The basal ganglia also provide the exploratory drive needed for navigation, foraging, and other reward-based or reinforcement learning⁵⁴, though little is known regarding the neurobiological mechanisms of exploratory behavior. Seminal work from O’Keefe and Nadel highlighted the relationship between exploration and spatial memory, a largely hippocampus-dependent function⁵⁵. Experimental models of middle cerebral artery occlusion (focal ischemic stroke) suggest the injury causes exploratory hyperactivity^{56,57}, which aligns with the role of spatial memory in exploration and the vulnerability of hippocampal neurons to ischemic injury. Without habituation facilitated by the hippocampus, animals may feel compelled to increase exploration, leading to duplication of exploration efforts for example. However, this behavioral abnormality hasn’t been explored in the context of CA-associated HIBI, and behavioral responses to ischemia are influenced by other external factors such as lighting⁵⁸ and time after the injury⁵⁹.

Recent evidence highlights zolpidem, otherwise known as Ambien, as an effective therapy to treat post-HIBI symptoms. Commonly used as a hypnotic/sedative agent, zolpidem is a GABA_A receptor agonist with a high selectivity for those expressing the $\alpha 1$ subunit. The distribution of these receptors throughout the basal ganglia allow them to exert a direct influence on striatal DA neurotransmission and thalamocortical signaling. Under normal conditions, zolpidem induces hypnotic effects by suppressing thalamocortical signaling via its action on tRN GABA_A- $\alpha 1$ -receptors. However, paradoxical effects on arousal after zolpidem administration have been described in clinical case studies of severe trauma^{60,61} and CA-induced HIBI^{62–65}. It’s administration has also been linked to improvement in Parkinson’s associated movement disorders^{66,67}.

Though it’s mechanism is largely theoretical⁶⁸, systemic zolpidem may ameliorate HIBI-associated behavioral impairments by partially replacing the function of striatal MSNs (i.e.

GABAergic striatal outflow). GABA_A- α -1 receptors are expressed in the striatum, GP, SNpr, and the tRN⁶⁹. As such, systemic zolpidem administration may normalize striatal outflow and thus GP outflow as well. As increased pallidal outflow after HIBI disinhibits SNpc DAergic neurons and drives post-CA striatal hyperdopaminergia, normalizing the neuronal firing of the striatal-pallidal circuitry may normalize SNpc DAergic neurons and reverse striatal hyperdopaminergia, as seen in figure 4. Though HIBI results in amplified GPi inhibitory drive which would presumably suppress thalamocortical signaling, animal models show elevated thalamocortical neuronal firing after CA_{70,71}. Zolpidem's actions on the high concentration of GABA_A- α -1 receptors in the tRN may normalize inhibitory drive on the intralaminar thalamus and ameliorate post-HIBI DoC.

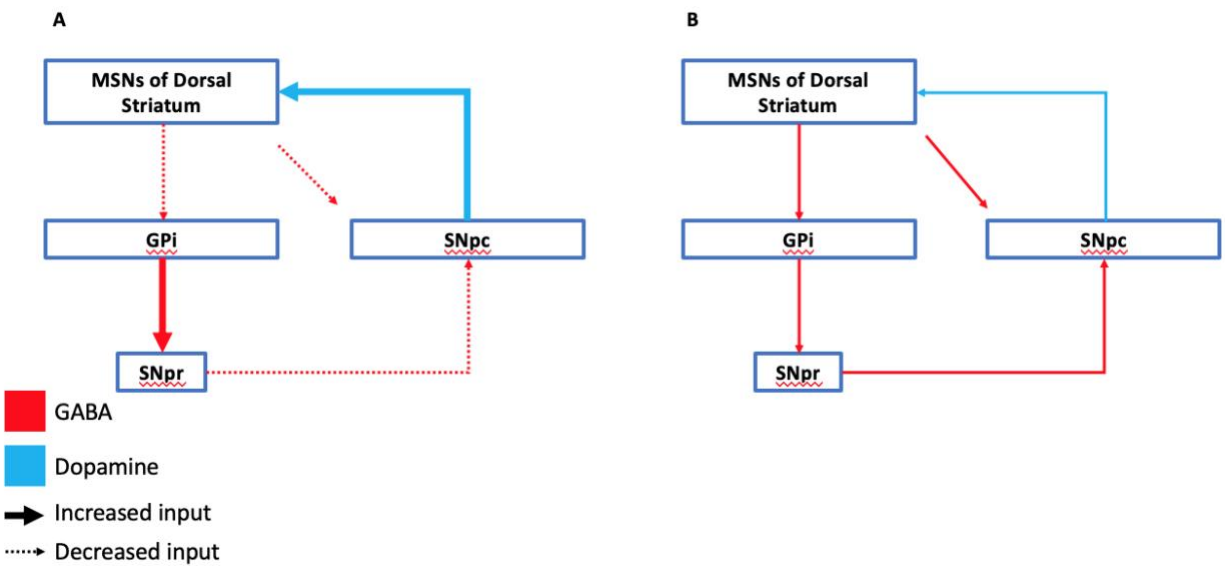


Figure 4: Mechanistic theory of HIBI-affected striatal-pallidal-nigral circuitry before (A) and after (B) systemic zolpidem administration.

(B) Systemic zolpidem administration may normalize striatal GABAergic outflow by acting on striatal GABA_A- α -1 receptors. Increased MSN outflow to the SNpc and GP may directly and indirectly increase inhibitory drive onto SNpc DAergic neurons, thus reversing striatal hyperdopaminergia.

Zolpidem treatment, however, has highly mixed results within the clinical population^{72–76}. Given the broad and heterogeneous distribution of GABA_A- α -1 receptors. The neurological changes underlying post-HIBI symptoms are dynamic processes as well. Taken with the idea that these regions interact within various closed loop circuits and influence a variety of basal ganglia-driven behaviors, zolpidem may exert vastly different downstream effects depending on where it binds its receptor.

This thesis aimed to elucidate the value of acute neurological and physiological readouts, as defined by neurological deficit scores, blood lactate values, and blood acid/base excess (ABE) values, in identifying heterogeneity among a population of animals which underwent a 5-min ACA injury model. The degree to which these acute readouts aligned with long-term behavioral, as well as neurological outcomes as indicated by DA neurotransmission findings from FSCV, was also evaluated.

Subsequently, the effects of chronic, systemic zolpidem administration on normalizing DA kinetics and behavioral abnormalities were assessed in comparison to untreated ACA animals. It was hypothesized that chronic zolpidem administration would ameliorate HIBI—induced behavioral deficits and reverse striatal hyperdopaminergia after ACA. Further, a cohesive conceptual framework, methodology, and technical feasibility plan was developed to test the impacts of regional zolpidem microinjections in the GPe, a key area in the regulation of controlled movement and consciousness that has dense expression of GABA_A- α -1 receptors.

2.0 Methods

Asphyxial Cardiac Arrest Model

Rats (n=56) were randomly selected to undergo the 5-min ACA model or sham procedure. Rats were housed in pairs prior to surgical procedures and were allowed unrestricted access to food and water as well as a 12-hr light/dark cycle, then were housed alone following recovery from the surgery. Those assigned to the ACA or sham group underwent procedures as described previously⁷. In brief, adult male Sprague-Dawley rats (350-400g; Envigo, Frederick, MD, USA) were housed for at least 3 days before the experiment under 12-h light/dark cycle with unrestricted access to food and water. On the day of the experiment, rats were anesthetized with isoflurane 4% in inspiration fraction of Oxygen (FiO₂), intubated with a 14 gauge intravenous catheter (Becton Dickinson, Sandy, UT, USA) and mechanically ventilated (Harvard Rodent Ventilator 683, Harvard Apparatus, South Natick, MA, USA; tidal volume 6 ml/kg, initial respiratory rate 40/min, positive end-expiratory pressure 5 cm H₂O FiO₂ 0.5), while held at euthermia by an overhead lamp and heating pad. Anesthesia was maintained with isoflurane 2%. Left femoral artery and vein were cannulated with polyethylene (PE) tubing (PE60 and PE90, respectively, Masterflex, Barnant, IL, USA) for blood pressure monitoring and drug administration, respectively, via surgical cutdowns. Baseline arterial blood gas (ABG) was obtained to assess acid-base balance and hematologic parameters with glucose and lactate.

Rats assigned to the ACA group received the following additional treatment: After 5-minute ACA induced by disconnection from the ventilator, epinephrine (50 µg/kg) and bicarbonate (1 mmol/kg) were given intravenously at the start of CPR. Additional epinephrine (25 µg/kg) was given 60s after the start of CPR. Resuscitation was performed via mechanical ventilation (FiO₂

1.0, identical respiratory parameters as above) and manual chest compression (300/min) until return of spontaneous circulation (ROSC). If ROSC was not achieved within 2 min of CPR, rats were defibrillated (Zoll 3M, Chelmsford, MA, USA; 10 J biphasic shock between sternal and esophageal electrode positioned behind the heart); defibrillation attempts were repeated if needed every 30 s during ongoing CPR. Sham rats received all surgical procedures except those directly associated with ACA and resuscitation under isoflurane anesthesia (1% with FiO₂ identical to the corresponding stage of the ACA protocol).

Post-Resuscitation Care

Arterial blood gases were obtained at 5-min post-ROSC, 30-min (prior to weaning from the ventilator) and 60-min (after weaning from the ventilator) post-ROSC. Rats were weaned from the ventilator at 30-min after ROSC, allowed to breathe spontaneously via endotracheal tube with supplemental oxygen delivered via nose-cone mask at 2L/min. Using a midline laparotomy incision, a Mini-Mitter probe (Mini-Mitter Co., Sunriver, OR, USA) was inserted into the peritoneal cavity to allow post-operative temperature control and continuous monitoring of vital functions. Rats were extubated 60 min after ROSC following decannulation. Then, rats were placed in cages and kept normothermic using an overhead heating lamp and/or a fan for 18 h in addition to supplemental oxygen (2L/min for 18 h) and unlimited access to food and water. The Mini-Mitter probe was removed 24 h later under brief isoflurane anesthesia using a nose-cone mask. Rats were then moved to the housing facility with a 12 h dark/light cycle, and unlimited access to standard food and water. Rats were housed individually in a standard environment. Neurological function was assessed daily for the first 3 days using an Overall Performance Category (OPC) score (1 = normal - ambulating, eating, drinking; 2 = mild disability - as OPC 1 but with abnormal sensory or motor function; 3 = moderate disability - responds to pain, no

ambulation, no righting, no eating or drinking, conscious; 4 = severe disability - no ambulation, no righting, no eating or drinking, comatose; 5 = death)⁷⁷ and a modified Neurologic Deficit Score (NDC; 0 - 10% = normal, 100% = maximum deficit)^{78,79}.

Acoustic Startle Response (ASR)

To assess HIBI-induced changes in the acoustic startle response and pre-pulse inhibition (PPI), ASR was performed one day before, as well as 3 days post-ACA or sham surgery. Each rat was placed in a Panlab Startle and Fear Conditioning Chamber using Packwin V.2.0 software and exposed to pseudorandomized intertrial 15 - 35 second white noise bursts at 85 dB, 95 dB, and 105 dB occurring over approximately 15 minutes following a 10 minute period of habituation (Harvard Apparatus, Holliston, MA, USA). 8 bursts occurred at each volume for a total of 24 bursts. The mean of maximum startle response amplitude (%) was calculated as a percentage for each of the three volume noise bursts. The percent (%) change of startle response of baseline compared to day 3 post-ACA or sham surgery.

Myoclonus Testing

Myoclonus testing occurred on D2 post-ACA or sham surgery. Rats were placed in a black receptacle (16" x 10" x 24") and were exposed to metronome (Korg, Tokyo, Japan) clicks at 95 dB volume over 60 seconds at a frequency of 45 beats per minute or 45 total clicks through an amplifier (Peavy, Meridian, MS, USA) located directly adjacent to the testing container following a 10 min habituation period in the black receptacle. Experiments were recorded using a digital video camera (Canon, Huntington, NY, USA). Graders blinded to the treatment group later watched the videos at reduced speed and assigned a categorical score for each of the 45 clicks: 1 = no reaction, 2 = startle reaction, 3 = Myoclonic reaction, 4 = stereotypy reaction. The average number of myoclonic responses for each treatment group were calculated.

Open Field Testing

Open field testing (OFT) was performed 7 days post-ACA or sham procedure. Following a 30 minute period of habituation in the testing room, rats were placed at the center of the open field apparatus (36.5”x 36.5” x 16”) facing the back wall and tracked using ANYMAZE software (Stoelting, Wood Dale, IL, USA) for the entire 600 seconds of the test. The measurements recorded included the total distance travelled (m), exploratory zone time allocation (%), and peripheral zone time allocation (%).

Sucrose Preference Testing (SPT)

Beginning 3 days post-ACA or sham procedure, rats were habituated with one bottle of 1% sucrose solution and one identical bottle of normal water. The position of these bottles (left or right) was switched until day 6, when two bottles of normal water were presented. On day 7 at 3:00 PM, rats were deprived of all fluid for 18 hours. At 8:00 AM the following day, 100 mL of tap water and 1% sucrose water were presented to rats for 1 hr in a quiet location. Consumption was measured at the end of the experiment and preference for sucrose water (%) was calculated by dividing the volume of sucrose water consumed by the total volume of water consumed.

Fast Scan Cyclic Voltammetry

Two weeks following ACA / Sham procedures, rats underwent fast scan cyclic voltammetry to measure regional variations of DA neurotransmission as described previously.⁵ In brief, rats were anesthetized with urethane (1.3 g/kg), mounted onto a stereotaxic apparatus and maintained at 37°C with a homeothermic blanket (Harvard Apparatus, Holliston, MA, USA). Midline incisions were made and soft tissues lifted to expose the skull to drill burr holes for the placement of microelectrodes. Carbon fiber microelectrodes (CFE) were fabricated as described previously.⁸⁰ Immediately prior to use, electrodes were electrically pretreated with a 70 Hz

biphasic cyclic waveform (0V→2V→0V) to enhance DA sensitivity. One recording microelectrode was inserted using flat skull coordinates (in mm) into the dorsal striatum [anterior posterior (AP): +1.0, mediolateral (ML): +3.0, and dorsoventral (DV): -4.6]⁸¹. A reference electrode was placed on the proximally exposed brain tissue to create a salt bridge. A bipolar stimulating electrode (MS301-1; Plastics One, Roanoke, VA, USA) was inserted into the median forebrain bundle (AP: -4.3, ML: +1.6, DV: -6.6)⁸¹.

Biphasic 60 Hz, 5 s (280 μ A amplitude and 2 ms pulse width) stimulations of the median forebrain bundle were used to evoke DA overflow. DA responses were electrochemically detected by the CFEs to which a triphasic cyclic voltage waveform (0V>1V>0.5V>0V) was applied at a rate of 400 V/s every 100 ms, using TarHeel CV software (ESA, Chelmsford, MA, USA). The stimulating electrode was advanced 200 μ m every 5 min until a DA signal was detected and then lowered 100 μ m every 10 min until a peak signal amplitude was obtained in the CFE. Experimental DA responses were then obtained using alternating 60- and 40 Hz stimulations for 2, 5 or 10 seconds according to the schematic depicted in Figure 1.

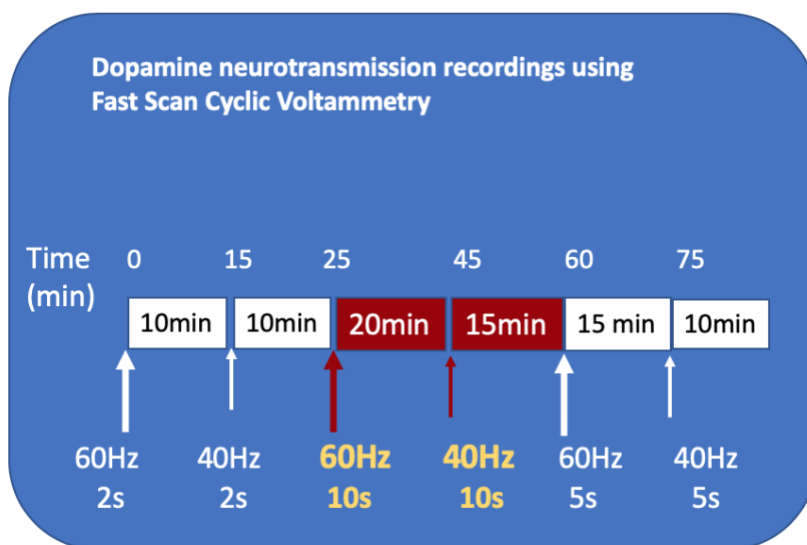


Figure 5: Schematic outlining FSCV experimental design and median forebrain bundle stimulation sequence.

Following *in vivo* electrode measurements, electrodes were calibrated with seven DA concentrations in artificial cerebrospinal fluid (pH = 7.2) composed of (in mM): 1.2 CaCl₂, 2.0 Na₂HPO₄, 1.0 MgCl₂, 2.7 KCl, and 145 NaCl₈₀. The DA concentration versus current calibration using a quadratic regression, which was then used to convert experimental DA responses from measured currents to DA concentrations.

Interpretation of DA Responses

DA response shapes were assessed by evaluating peak DA concentrations associated with experimental DA response amplitudes, or evoked overflow (EO) [DA].

As validated and used in previous studies, we implemented the quantitative neurobiological (QN) framework to model kinetic parameters onto DA responses to 60 Hz, 10 and 5 s stimulations obtained from ACA and Sham rats.⁸⁰ The QN framework was used for characterizing DA release and reuptake in lieu of the classic Michaelis-Menten (M-M) model⁸² because it does not assume constant DA release rate or a constant reuptake efficiency and affinity for DA on the part of DAT. The equations and terms used in the QN model to describe release and reuptake components of stimulated DA responses can be found in Table 1. Briefly, DA release rate during stimulation (DAR_{stim}) is described by equation 1 as an exponential decay function with a time constant of $\Delta DAR\tau$ and a steady-state release rate (DAR_{ss}). Post-stimulation DA release rate (DAR_{post}) is described in equation 2 as release rate that decreases biphasically after stimulation ends, with a rapid exponential and prolonged linear decay components. Lastly, reuptake kinetics were modeled similarly to the M-M model, except K_m was defined as a dynamic term that increases during stimulation according to the logistic function in equation 3 to model a decreasing reuptake efficiency caused by the stimulation itself.

Table 1: Equations and parameters utilized in stimulations.

<i>DA release rate (during stimulation):</i>	
$DAR_{stim}(t) = \Delta DAR * e^{-t_{stim}/\Delta DAR\tau} + DAR_{SS}$ (Equation 1)	ΔDAR DA release rate undergoing decay
	$\Delta DAR\tau$ Time constant of release
	DAR_{SS} Steady-state DA release rate
<i>DA release rate (post-stimulation):</i>	
$DAR_{post}(t_{post}) = X_R * DAR_{ES} * e^{-\frac{t_{post}}{\tau_R}} + (1 - X_R) * DAR_{ES} - m * t_{post}$ (Equation 2)	X_R Rapid release fractional component
	DAR_{ES} DA release rate at end of stimulation
	τ_R Time constant of rapid release component
	m Linear decay slope of prolonged release component
<i>DA reuptake rate:</i>	
$ReuptakeRate(t) = \frac{V_{max}}{\frac{K_m(t)}{[DA]} + 1}$	V_{max} Maximal reuptake rate
	$K_m(t)$ M-M constant (an inverse measure of efficiency)
where,	
$K_m(t) = K_{mi} + \Delta K_m \left(1 - \frac{1}{1 + \frac{t}{K_{m_{inf}}^k}} \right)$ (Equation 3)	K_{mi} Initial K_m
	ΔK Magnitude of change in K_m dynamics
	$K_{m_{inf}}$ Time of inflection of K_m dynamics
	k Measure of the steepness of the inflection in K_m dynamics

The simulations produced estimates of DA release and reuptake rates over the time course of stimulated DA responses. Specifically, we examined four parameters that were derived from these simulations to characterize the effects of ACA on stimulated DA neurotransmission: K_{mi} , V_{max} , initial DA release rate (DAR_i), and DA released. K_{mi} describes the M-M constant that estimates the efficiency of DAT molecules at physiological conditions, and V_{max} is an estimate of maximum reuptake rate that depends upon local DAT density and efficiency. As DA release is a dynamic process during stimulation, we provided estimates of DAR_i and total estimated DA released during stimulation by integrating DA release rate equations over the stimulation duration.

Zolpidem Administration

Zolpidem was dissolved in DMSO, vortexed until fully dissolved, and then dissolved into 0.1M PBS to bring the solution to 20% total DMSO. Animals received daily intraperitoneal injections of either 0.1mg/kg (n=5) or 0.2mg/kg (n=5) zolpidem solution were performed starting at D2 post-ACA until D14 post-ACA. This dosing range was shown to improve DA dysregulation-driven motor impairments in PD-relevant animal models (Assini and Abercrombie, 2018). Due to COVID-19 shutdown, no Sham animals were treated with zolpidem, nor ACA animals with chronic vehicle (0.1M PBS) injections. For evaluating behavioral outcomes, the effects of chronic zolpidem administration were evaluated for low and high dose groups combined as well as separately for the high dose zolpidem animals.

Injury Severity Metrics

NDS were assigned 1, 2, and 3 days post-injury, as well as on the final day of the study (D7 or D14 post-injury). Blood Lactate and ABE values were obtained at baseline as well as 5, 30, and 60 minutes post-resuscitation. To qualitatively assess bimodal distribution between injury and sham groups, as well as score range and distribution over time, histograms and scatterplots were generated for NDS, lactate values, and ABE values. The median of D1 – D3 NDS were used for all subsequent analyses. The median among 5-, 30-, and 60-minute post-resuscitation values were used for all subsequent analyses.

Statistical Analyses

All statistical analyses were performed using either statistical analysis software (SAS) version 9.4 (Cary, NC, USA), Rstudio software version 3.5 (Corvallis, OR, USA), or Graphpad Prism version 8 (San Diego, CA, USA). Differences were considered statistically significant if $p < 0.05$, unless otherwise stated.

Cox Regression for Survival Analysis

In order to investigate the effect of NDS, blood lactate, and blood ABE values on the time exclusion from the study, either by death or distress, takes to happen, a Cox regression was performed among all ACA animals (n=30). To account for varied range between NDS, lactate, and ABE, their values were standardized by subtracting the mean and dividing by the standard deviation.

Correlation Analyses

Spearman's correlations were performed to examine associations among NDS, lactate values, and ABE values, as well as between these injury metrics and behavioral/dopamine-related outcomes. Kolmogorov-smirnov (K-S) normality tests were performed for all injury, behavioral, and dopamine-related metrics prior to correlations. Resulting p-values from K-S tests greater than 0.05 for any tested data were considered to have a normal distribution. Pearson's correlations were then performed for association pairs with normal distribution, whereas Spearman's rank correlations were performed for association pairs with abnormal distribution. Due to lack of normality across behavioral and dopamine-related metrics, only Spearman's rank correlations were performed. To evaluate associations between dopamine-related and behavioral testing outcomes, partial correlation analyses were performed with NDS, lactate values, and ABE values included as covariates. For all correlational analyses performed, mild associations ($p=0.1-0.199$, $r=\pm 0.3-0.499$) were labeled in orange, moderate associations ($p=0.01-0.09$, $r=\pm 0.5-0.699$) were labeled in green, and strong associations ($p<0.01$, $r=\pm 0.5-0.699$) were labeled in blue.

Analysis of Variance/Covariance

Analysis of variance (ANOVA) or analysis of covariance (ANCOVA) were performed to evaluate the differential effects of zolpidem on behavioral performance outcomes and dopamine-related outcomes, and how they compare to those of untreated ACA animals. Injury metrics which significantly correlated with the outcome-of-interest were used as covariates in the associated analysis. If no injury metrics were significantly correlated with the outcome-of-interest, ANOVA was performed. Post hoc pairwise comparisons were assessed using Tukey's test.

3.0 Results

Injury Metrics Outcome Change Over Time and Are Bimodally Distributed Between Injury and Sham Groups

To qualitatively assess bimodal distribution between injury and sham groups, as well as score range and distribution over time, histograms and scatterplots were generated for NDS (Figure 3a-3d), lactate values (Figure 4a-4d), and ABE values (Figure 5a-5d).

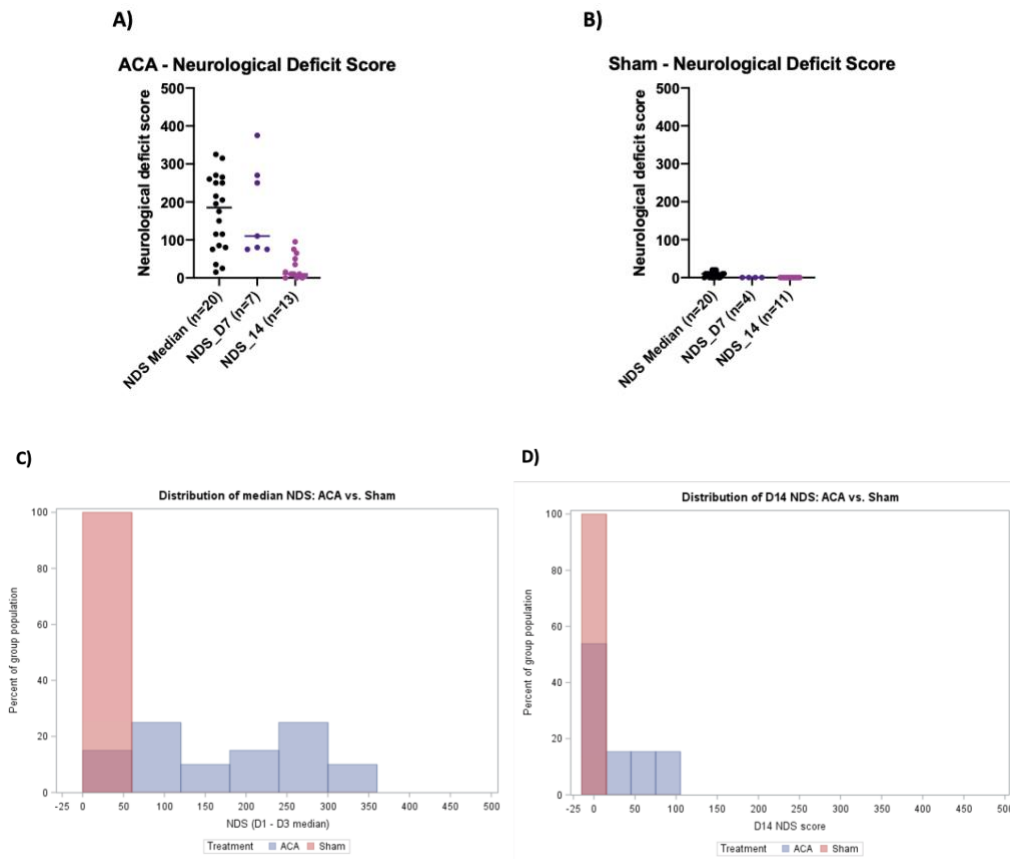


Figure 6: Scatterplots show blood lactate values for ACA (a) and Sham (b) groups at baseline, D1-D3 (median), D7 and D14 post-surgery.

Overlaid histograms show bimodal distribution between ACA and Sham groups for blood lactate at D1-D3 (median) (c) and D14 (d) post-surgery.

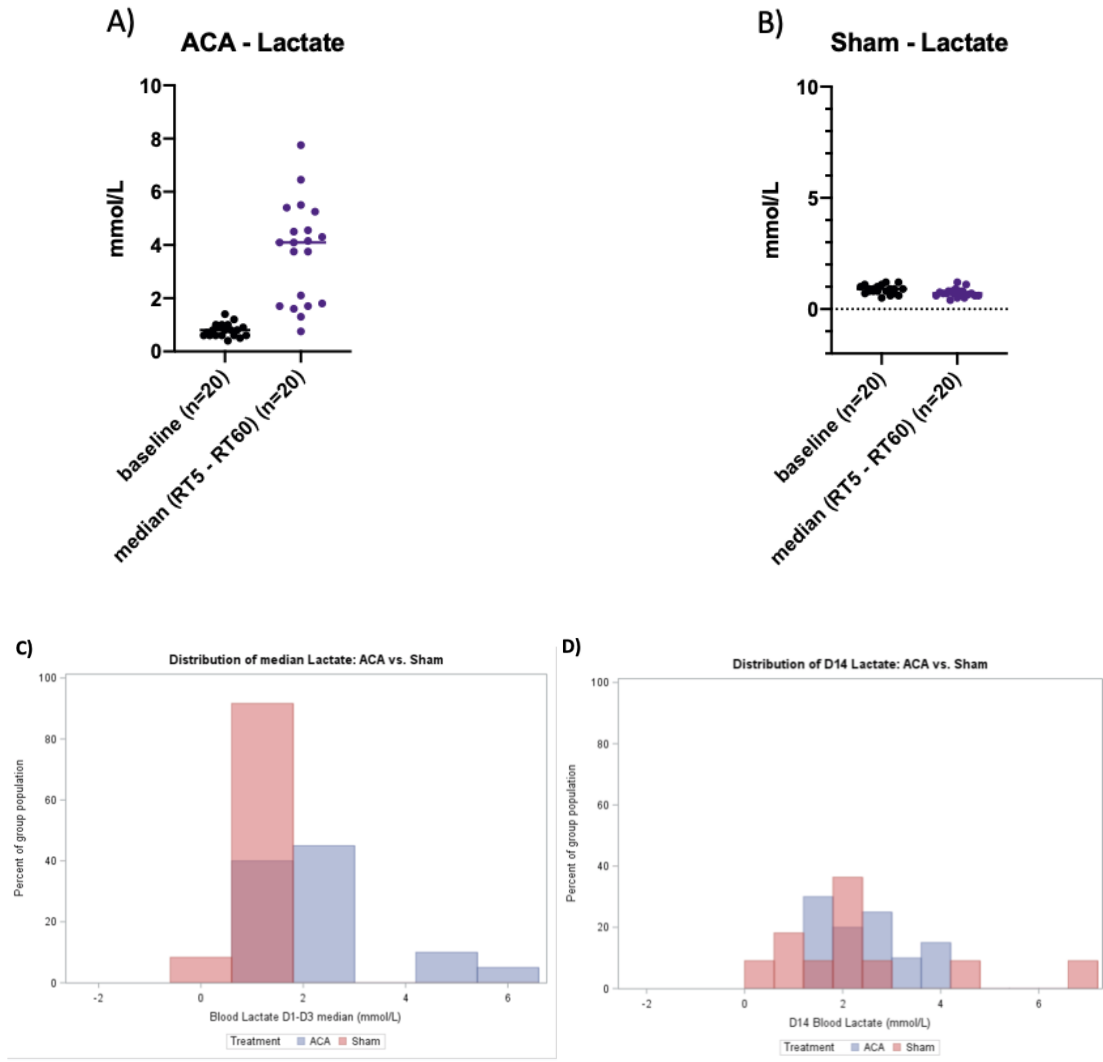


Figure 7: Scatterplots show blood lactate values for ACA (a) and Sham (b) groups at baseline, D1-D3 (median), D7 and D14 post-surgery.

Overlaid histograms show bimodal distribution between ACA and Sham groups for blood lactate at D1-D3 (median) (c) and D14 (d) post-surgery.

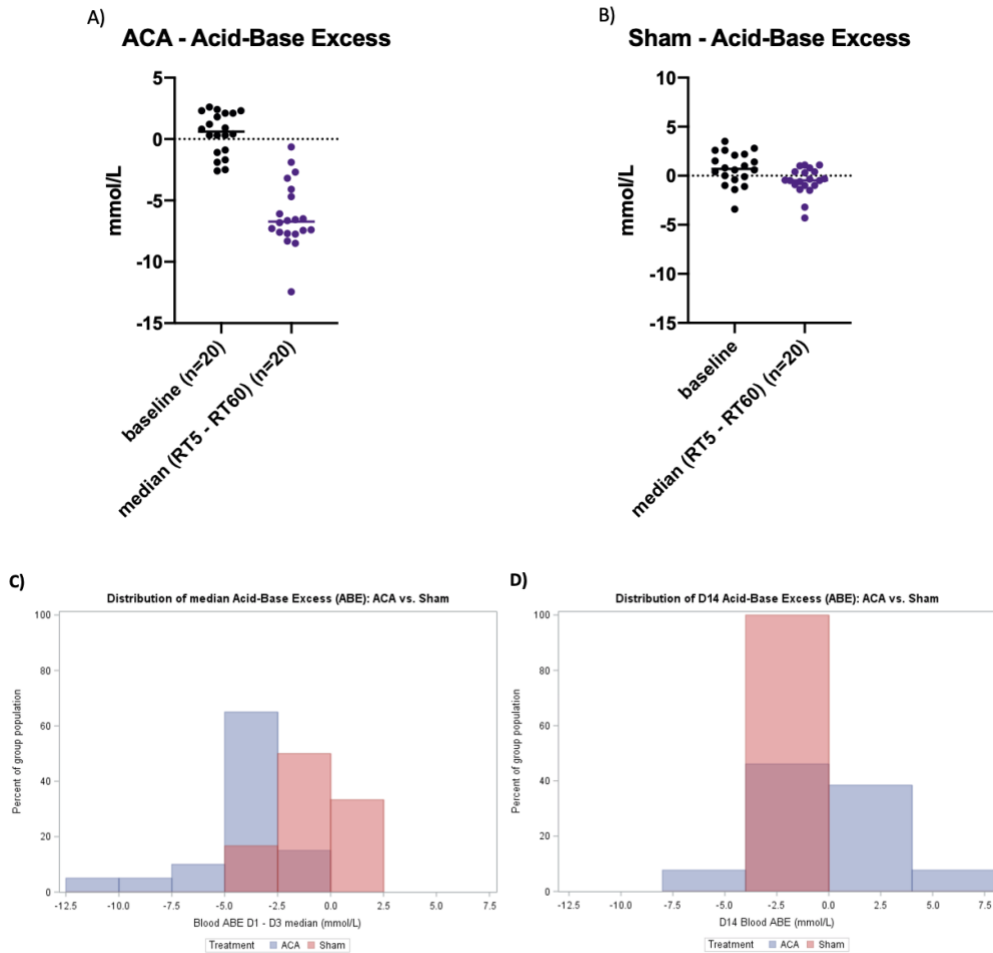


Figure 8: Scatterplots show blood acid-base excess (ABE) values for ACA (a) and Sham (b) groups at baseline, D1-D3 (median), D7 and D14 post-surgery.

Overlaid histograms show bimodal distribution between ACA and Sham groups for blood ABE at D1-D3 median (c) and D14 (d) post-surgery.

Acute NDS Predicts Survival After 5-Min ACA

NDS for days 1 – 3 post-injury were plotted for surviving ACA animals (Figure 6). Median scores dropped significantly from D1 to D2 post-injury and from D1 to D3 post-injury. Distribution of injury metrics outcomes were also assessed for ACA survivors vs. non-survivors (animals excluded from the study for death or distress) (Fig. 7a-7c). Median NDS for non-

survivors were significantly higher compared to their survivor counterparts (Fig. 7a), whereas median lactate (Fig. 7b) and ABE (Fig. 7c) values were not different between groups.

Neurological Deficit Score Distribution

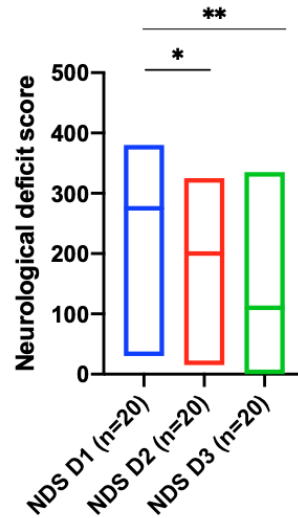


Figure 9: Median values for NDS at D1 – D3 post-injury, represented by bars, show acute neurological outcome after 5min ACA.

Paired t-tests showed a significant reduction in NDS from D1 to D2 (240.5 ± 21.98 vs. 173.8 ± 20.94 , $*p=0.0341$) as well as from D1 to D3 post-injury (240.5 ± 21.98 vs. 130 ± 24.6 , $**p=0.0018$).

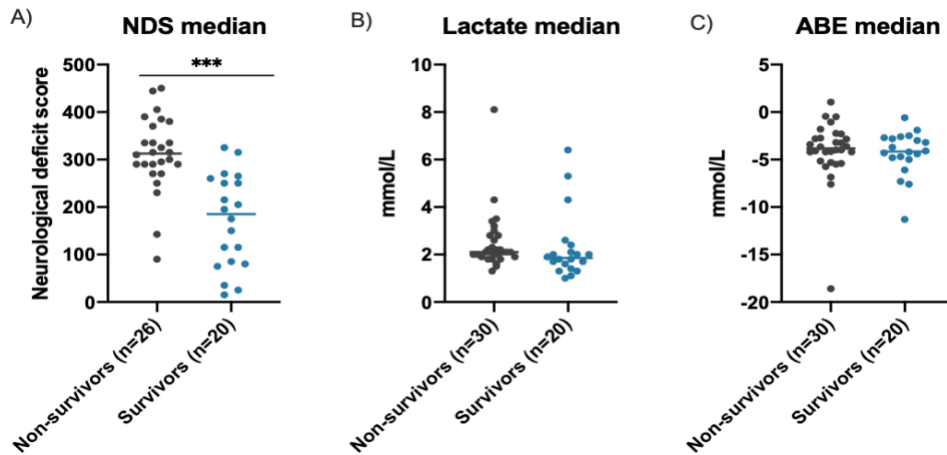


Figure 10: Scatterplots of NDS (a), lactate (b), and ABE (c) values show differences between survivors and non-survivors after ACA injury.

Median NDS for non-survivors were significantly higher compared to their survivor counterparts (Fig. 7a: 311.6 ± 15.73 vs. 171 ± 21.94 , *** $p < 0.0001$), whereas median lactate (Fig. 7b) and ABE (Fig. 7c) values were not different between groups.

To further explore the validity of NDS as a useful predictor of injury survival, a multivariable Cox regression was performed using median NDS, lactate values, and ABE values of animals that survived through the duration of the study and animals that were prematurely excluded (a.k.a. non-survivors) due to death or distress (Table 2). The model showed that only (standardized) NDS was significant, in that one standard deviation (SD) increase in NDS increased the hazards of rats being excluded from the study (via death or being out-of-protocol) by 5.205 times. For ABE and Lactate, the HR also increased with a 1-SD increase, but these covariates were not significant.

Covariates from the multivariable Cox model were also used to estimate/predict ACA animal survival probabilities up to a specific post-injury timepoints (Table 3). ACA animals had a 80.1% predicted survival rate up to D3 post-injury, whereas predicted survival rates up to D6 and D7 post-injury reduced to 67.7% and 52.1%, respectively (Table 3). Survival probability out

to D14 post-injury matched that for D7 because no rat was excluded from the study due to death or weight loss after 7 days in our data.

Table 2: Cox regression model of study exclusion (due to death/distress) on standardized NDS, lactate, and ABE median scores (n=45, number of events=25).

NDS significantly aligned with study exclusion (HR=3.958, *p<0.0001), but not lactate or ABE.**

Variable	Beta	SE	HR	P-value	95% CI for HR
Standardized NDS (D1-D3 median)	1.650	0.384	5.205	<0.0001	(1.4173, 11.053)
Standardized Lactate (5, 30, 60 mins median)	0.207	0.379	1.230	0.21177	(0.6931, 5.228)
Standardized ABE (5, 30, 60 mins median)	0.360	0.385	1.434	0.27376	(0.6369, 4.914)

Table 3: Median probabilities of ACA animals surviving to D3, D6, and D7 post-injury.

Days	Median survival probability [Q1-Q3]
3	0.910 [0.969-0.991]
6	0.793 [0.924-0.979]
7	0.614 [0.847-0.956]

Injury Metrics Correlate with Behavioral And Dopamine-Related Outcomes

Because Kolmogorov-smirnov tests revealed non-normal distribution of relevant data outcomes, spearman correlations were performed to evaluate associations among injury metrics (Table 4), between injury metrics and DA release-based outcomes (Table 5), DA reuptake-based outcomes (Table 6), and between injury metrics and behavioral outcomes (Table 7). NDS median values significantly correlated with long-term (D14 post-injury) NDS values (*p=0.0175, r=0.6565). NDS median values also correlated with median lactate (***p<0.0001, r=0.864) and median ABE values (**p=0.0006, r=-0.702).

Analyses showed moderate associations between NDS and all three ASR metrics, as well as both open field testing (OFT) metrics. NDS negatively correlated with Kmi as well. Lactate moderately correlated with all three ASR metrics as well as both OFT metrics. Additionally, Lactate inversely correlated with total DA released, initial DA release rate (DARi), and Kmi. ABE moderately correlated with all three ASR metrics, distance traveled during OFT, and sucrose preference testing (SPT). ABE also correlated with evoked DA overflow, total DA released, and DARi.

Table 4: Spearman’s rank correlations show associations between median NDS and D14 NDS, median lactate, and median ABE values.

Mild (r=+/-0.3-0.499; p=0.1-0.199), moderate (r=+/-0.5-0.699; p=0.01-0.099), and strong (r=+/- 0.7-0.999; p<0.01) correlations are shown in orange, green, and blue, respectively.

Injury metrics	P-value	spearman R
NDS median vs. NDS D14	0.0175	0.6565
NDS median vs. Lactate median	<0.0001	0.864
NDS median vs. ABE median	0.0006	-0.702

Table 5: Spearman’s rank correlations show associations between injury metrics and DA release-based metrics.

Mild ($r=+/-0.3-0.499$; $p=0.1-0.199$), moderate ($r=+/-0.5-0.699$; $p=0.01-0.099$), and strong ($r=+/- 0.7-0.999$; $p<0.01$) correlations are shown in orange, green, and blue, respectively.

DA release-based metrics	P-value	spearman R
NDS median vs. maximal evoked DA	0.6	0.1596
NDS median vs. evoked DA at 1s	0.8956	-0.04127
NDS median vs. total DA released	0.4281	-0.2393
NDS median vs. DARI	0.3688	-0.27
Lactate median vs. maximal evoked DA	0.8951	-0.04132
Lactate median vs. evoked DA at 1s	0.8095	0.07438
Lactate median vs. total DA released	0.1891	-0.3884
Lactate median vs. DARI	0.1394	-0.4331
ABE median vs. maximal evoked DA	0.7097	-0.1154
ABE median vs. evoked DA at 1s	0.1247	-0.4505
ABE median vs. total DA released	0.0208	0.6429
ABE median vs. DARI	0.0223	0.6355

Table 6: Spearman’s rank correlations show associations between injury metrics and DA reuptake-based metrics.

Mild ($r=+/-0.3-0.499$; $p=0.1-0.199$), moderate ($r=+/-0.5-0.699$; $p=0.01-0.099$), and strong ($r=+/- 0.7-0.999$; $p<0.01$) correlations are shown in orange, green, and blue, respectively.

DA reuptake-based metrics	P-value	spearman R
NDS median vs. Kmi	0.0225	-0.6356
NDS median vs. Vmax	0.3982	0.2667
Lactate median vs. Kmi	0.0197	-0.6477
Lactate median vs. Vmax	0.8617	-0.05624
ABE median vs. Kmi	0.6437	0.1404
ABE median vs. Vmax	0.433	0.2487

Table 7: Spearman’s rank correlations show associations between injury metrics and behavioral outcomes.

Mild ($r=+/-0.3-0.499$; $p=0.1-0.199$), moderate ($r=+/-0.5-0.699$; $p=0.01-0.099$), and strong ($r=+/- 0.7-0.999$; $p<0.01$) correlations are shown in orange, green, and blue, respectively.

Behavioral outcomes	P-value	spearman R
NDS median vs. ASR_85	0.0643	0.4214
NDS median vs. ASR_95	0.0211	0.5117
NDS median vs. ASR_105	0.0097	0.5636
NDS median vs. myoclonus	0.9811	-0.005654
NDS median vs. OFT_distance	0.0004	-0.8501
NDS median vs. OFT_exploratory zone entries	0.022	-0.6367
NDS median vs. sucrose preference	0.6921	-0.121
Lactate median vs. ASR_85	0.0321	0.4802
Lactate median vs. ASR_95	0.0071	0.5819
Lactate median vs. ASR_105	0.0277	0.4915
Lactate median vs. myoclonus	0.902	-0.02941
Lactate median vs. OFT_distance	0.0391	-0.584
Lactate median vs. OFT_exploratory zone entries	0.1286	-0.4449
Lactate median vs. sucrose preference	0.7259	0.1074
ABE median vs. ASR_85	0.0519	-0.4406
ABE median vs. ASR_95	0.0096	-0.5639
ABE median vs. ASR_105	0.0101	-0.5609
ABE median vs. myoclonus	0.7141	-0.08738
ABE median vs. OFT_distance	0.0473	0.5659
ABE median vs. OFT_exploratory zone entries	0.233	0.3561
ABE median vs. sucrose preference	0.1517	-0.4231

Dopamine Metrics and Behavioral Outcome Associations

To assess functional coupling between behavioral outcomes and DA neurotransmission outcomes, and to evaluate any confounding or mediating effects of the established injury severity metrics on these outcomes after ACA, partial correlation analyses were performed among ACA animals. ABE was found to be a negative confounder for two association pairs: ASR metrics significantly correlated with evoked DA overflow at 1s into electrical stimulation, and these associations were attenuated when covarying for ABE. Additionally, sucrose preference significantly correlated with maximal evoked DA and this association was strengthened by

covarying for ABE. Table 8 summarizes these association pairs which changed significantly after adjusting for ABE.

Table 8: Summary of association pairs from partial correlation analyses (Spearman’s rank correlations) which significantly changed after adjusting for ABE.

Mild ($r=+/-0.3-0.499$; $p=0.1-0.199$), moderate ($r=+/-0.5-0.699$; $p=0.01-0.099$), and strong ($r=+/- 0.7-0.999$; $p<0.01$) correlations are shown in orange, green, and blue, respectively.

VARIABLES	COVARIATE	unadjusted p	unadjusted r	adjusted p	adjusted r	more/less significant
ASR 85 vs. Evoked DA at 1s	ABE median	0.05815753	0.543956044	0.0995	0.49791	less
ASR_95 vs. Evoked DA at 1s	ABE median	0.129874411	0.445054945	0.3264	0.31021	less
Sucrose preference vs. Maximal evoked DA	ABE median	0.008603508	-0.708791209	0.0006	-0.84175	more

Effects of Chronic Zolpidem Administration on Restoring HIBI-Induced Behavioral Deficits

Injury metrics which significantly correlated with the outcome-of-interest after Spearman’s rank correlations were used as covariates in the associated analysis. If no injury metrics were significantly correlated with the outcome-of-interest, ANOVA was performed. Post hoc pairwise comparisons were assessed using Tukey’s test.

Acoustic Startle Response

Acoustic startle response (ASR) testing was performed to measure sensorimotor changes following HIBI on day 3 post-surgery. Untreated ACA rats showed exaggerated acoustic startle responses across all sound burst intensities (Fig. 8a, 8b, 8c) compared to Sham rats 3 days following surgery. While the ACA group showed increased responses, Sham responses decreased compared to their baseline scores. The combined group of low- and high-dose zolpidem-treated zolpidem-treated rats (0.1mg/kg and 0.2mg/kg, respectively) did not show normalized responses except for the 105-dB sound bursts when combined, wherein zolpidem animals were not significantly different from Sham nor untreated ACA animals (Fig. 8a-8c). High dose (0.2mg/kg)

zolpidem-treated rats, when evaluated on their own (Fig. 8d-8f), exhibited significantly lower responses for 95-dB and 105-dB sound bursts compared to untreated ACA animals (Fig. 8e-8f).

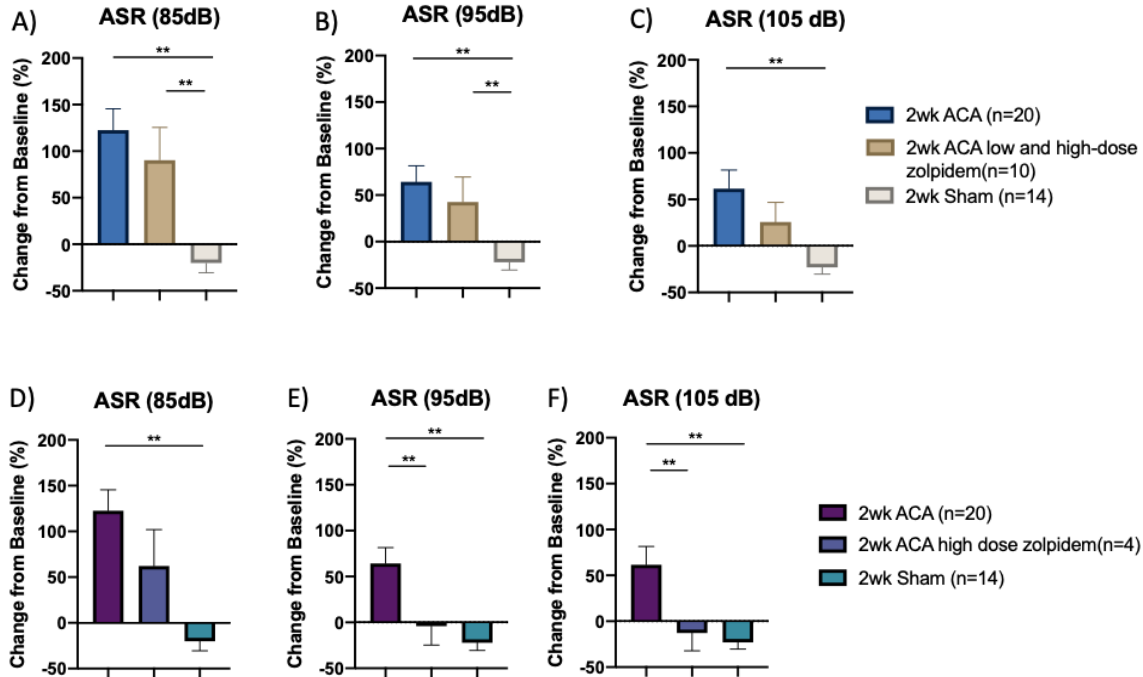


Figure 11: Mean ± SEM for acoustic startle responses at 85 dB (8a, 8d), 95 dB (8b, 8e), and 105 dB (8c, 8f) sound bursts shown as a percent change from baseline to 3 days post-surgery.

(a) ANCOVA showed a main effect of group (** $p=0.0009$), but no effect of NDS median, lactate median, or ABE median. Post hoc Tukey's test show significant differences between 2wk ACA and 2wk Sham groups (** $p=0.0002$). (d) ANCOVA showed a main effect of group (** $p=0.0009$), but no effect of NDS median, lactate median, or ABE median. Post hoc Tukey's test show significant differences between 2wk ACA and 2wk Sham groups (** $p=0.0002$), as well as between 2wk ACA ambien and 2wk Sham groups ($p=0.0365$). (b) ANCOVA showed a main effect of group (** $p=0.0065$), but no effect of NDS median, lactate median, or ABE median. Post hoc Tukey's test show significant differences between 2wk ACA and 2wk Sham groups (** $p=0.0017$), as well as between 2wk ACA ambien and 2wk Sham groups ($p=0.0221$). (e) ANCOVA showed a main effect of group (** $p=0.0065$), but no effect of NDS median, lactate median, or ABE median. Post hoc Tukey's test show significant differences between 2wk ACA and 2wk Sham groups (** $p=0.0017$) as well as

2wk ACA and 2wk ACA ambien group (*p=0.0128). (c) ANCOVA showed a main effect of group (*p=0.0246), but no effect of NDS median, lactate median, or ABE median. Post hoc Tukey's test show significant differences between 2wk ACA and 2wk Sham groups (**p=0.0015). (f) ANCOVA showed a main effect of group (*p=0.0246), but no effect of NDS median, lactate median, or ABE median. Post hoc Tukey's test show significant differences between 2wk ACA and 2wk Sham groups (**p=0.0007), as well as 2wk ACA and 2wk ACA ambien group (*p=0.0147).

Myoclonus Testing

Myoclonic responses were measured at day 2 post-surgery for untreated ACA, zolpidem-treated ACA, and Sham animals (Figure 9). Untreated ACA rats showed a marked increase in the percent of myoclonic response compared to Sham group. Neither zolpidem-treated group showed a reduction in myoclonic responses compared to untreated ACA animals (Figure 9a,9b).

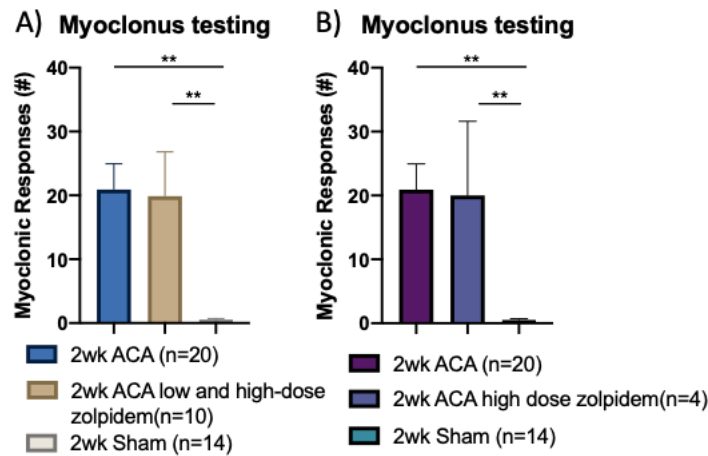


Figure 12: Mean \pm SEM values for myoclonic responses observed D2 following ACA/sham surgery.

(a) ANOVA showed significant differences across groups (**p=0.0025). Post hoc Tukey's test showed significant differences between 2wk ACA and 2wk Sham groups (**p=0.0014), as well as between 2wk Sham and 2wk ACA ambien groups (**p=0.0048). (b) ANOVA showed significant differences across groups (**p=0.0025). Post hoc Tukey's test showed significant differences between 2wk ACA and 2wk Sham groups (**p=0.0007), as well as between 2wk Sham and 2wk ACA ambien groups (**p=0.016).

Open Field Testing

Mobility (Figure 10) and exploratory behavior (Figure 11) were assessed via open field testing (OFT) on day 7 post-ACA/Sham surgery for untreated ACA, zolpidem-treated ACA, and Sham animals. ACA significantly reduced both the distance traveled (Fig. 10) and number of entries to the exploratory zone (Fig. 11) compared to Sham animals. The combined group of low and high dose zolpidem-treated animals showed no significant improvements in the distance traveled (Fig. 10a) nor exploratory zone entries compared to untreated ACA animals (Fig. 11a). High dose zolpidem-treated animals exhibited a modest increase in the distance traveled (Fig. 10b), though also not different from shams. Additionally, the high dose zolpidem group showed a slight reduction in exploratory zone entries compared to untreated ACA animals, though not significant (Fig. 11b).

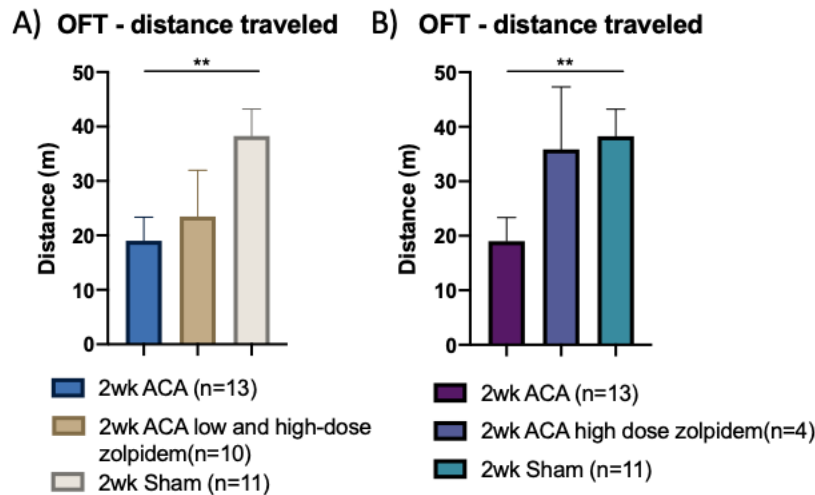


Figure 13: Mean \pm SEM values for distance traveled in the OFT D7 post-surgery.

(a) ANCOVA showed a main effect of group ($*p=0.0264$) as well as a main effect of NDS median ($**p=0.0021$). Post hoc Tukey's test show significant difference between 2wk ACA and 2wk Sham group ($*p=.0192$). (b) ANCOVA showed a main effect of group ($**p=0.0088$) as well as a main effect of NDS median ($**p=0.0053$). Post hoc Tukey's test show significant difference between 2wk ACA and 2wk Sham group ($*p=.0103$).

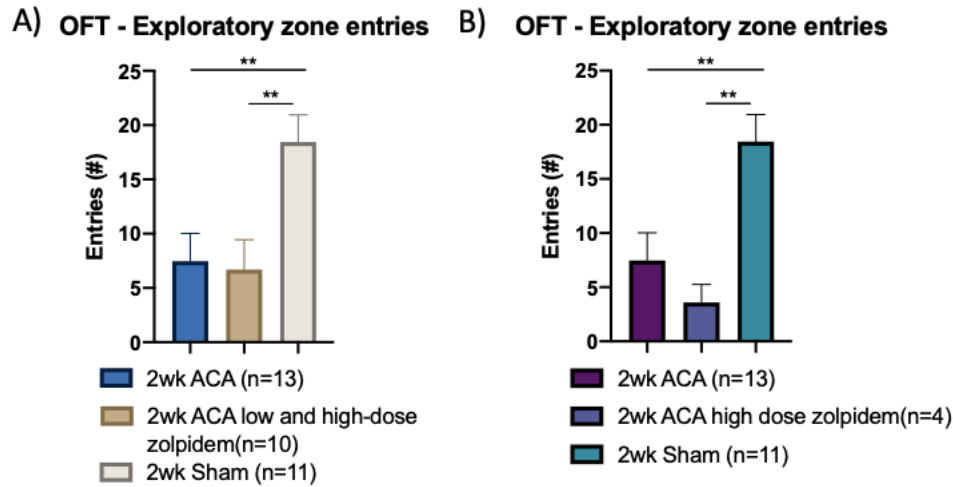


Figure 14: Mean \pm SEM values for exploratory zone entries in the open field D7 post-surgery.

(a) ANCOVA showed a main effect of group (** $p=0.0058$) as well as a main effect of NDS median ($p=0.03$).

Post hoc Tukey's test show significant difference between 2wk ACA and 2wk Sham group (** $p=.0046$), as well as between 2wk ACA ambien and 2wk Sham groups (** $p=0.0045$).

(b) ANCOVA showed a main effect of group (** $p=0.0011$) as well as a main effect of NDS median ($p=0.0115$). Post hoc Tukey's test show significant difference between 2wk ACA and 2wk Sham group (** $p=.0032$), as well as between 2wk ACA ambien and 2wk Sham groups (** $p=0.0025$).

Sucrose Preference Testing

To assess anhedonia after ACA, sucrose preference testing (SPT) was performed on day 8 post-ACA/sham surgery for untreated ACA, zolpidem-treated ACA, and Sham animals. ACA caused a significant decrease in sucrose preference which was reversed in the high dose zolpidem-treated animals (Fig. 12b). The combined group of low and high dose zolpidem-treated animals was not significantly different from Sham nor untreated ACA animals (Fig. 12a).

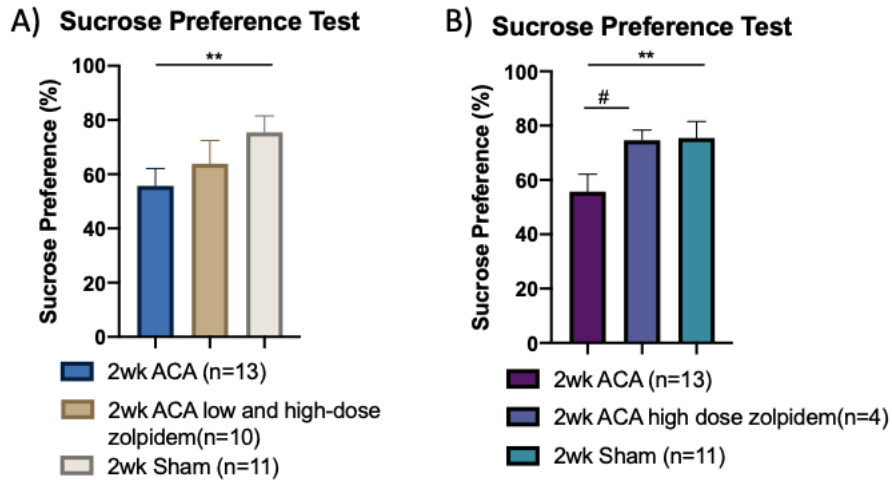


Figure 15: Mean \pm SEM of sucrose preference calculated on D8 post-surgery.

(a) ANCOVA showed no main effect of group, though it did show a main effect of ABE median (* $p=0.0327$).

Post hoc Tukey's test showed a significant difference between 2wk ACA and 2wk Sham groups (* $p=0.0482$).

(b) ANCOVA showed a main effect of group (* $p=0.0477$) and a slight main effect of ABE median ($p=0.0517$).

Post hoc Tukey's test showed a significant difference between 2wk ACA and 2wk Sham groups (* $p=0.0428$)

and a trend towards differences between 2wk ACA and 2wk ACA ambien groups (# $p=0.088$).

Effects of Chronic Zolpidem on Voltammetric Responses and Evoked DA Overflow in The Dorsal Striatum After ACA-Induced HIBI

For all voltammetric data, the low and high dose zolpidem-treated animals were combined into one group. Electrically stimulated DA responses reflect a balance of DA release and reuptake kinetics. Figure 13 shows the average DA responses in the dorsal striatum (D-STR) for untreated ACA, zolpidem-treated ACA, and Sham animals following a maximal 60 Hz, 10 s stimulation of the medial forebrain bundle (MFB). Responses were obtained at day 14 post-ACA/Sham surgery. Maximal evoked DA overflow was significantly increased during and after stimulation in the ACA group compared to the Sham group at 2 weeks post-surgery (Fig. 13a). Chronic zolpidem administration seemed to reduce maximal evoked DA in that treated animals were not significantly

different from untreated ACA nor Sham groups (Fig. 13a). Evoked DA at 1s into the stimulation was also assessed among groups, though ANCOVA showed no significant differences (Fig. 13b).

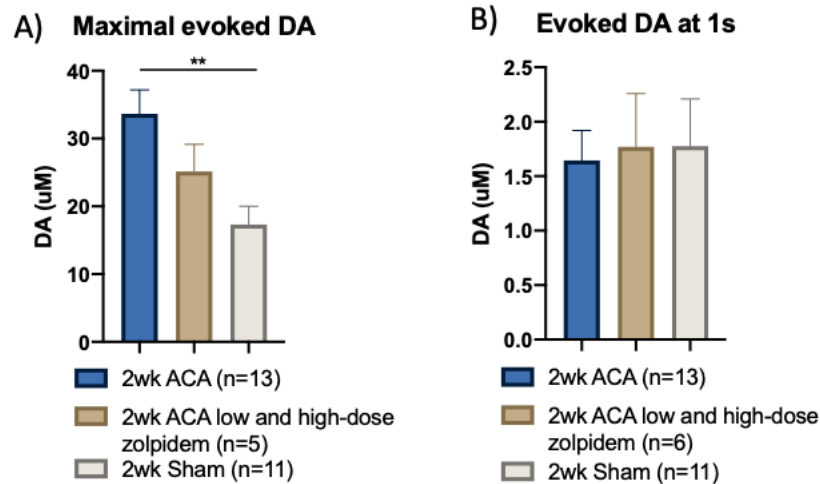


Figure 16: Mean ± SEM of maximal evoked DA overflow (a) and evoked DA overflow 1s into stimulation (b) in the D-STR following 60Hz, 10s MFB stimulations two weeks post-surgery.

(a) ANOVA showed significant main effect of group ($p=0.0044$). Post hoc Tukey's test showed significant difference between 2wk ACA and 2wk Sham groups (** $p<0.01$). (b) ANCOVA showed no significant differences across groups.

Effects of Chronic Zolpidem on ACA-Induced DA Kinetics Alterations

In order to measure DA kinetics in the D-STR, FSCV data were modeled using the QN framework as described previously described. Figure 14 shows group comparisons for DA release-based metrics for untreated ACA, zolpidem-treated ACA, and Sham animals at day 14 post-ACA/Sham surgery. QN simulations revealed that total [DA] release (Fig. 14a), initial DA release rate (DAR_i) (Fig. 14b), were significantly increased in both untreated and zolpidem-treated ACA groups compared to Shams.

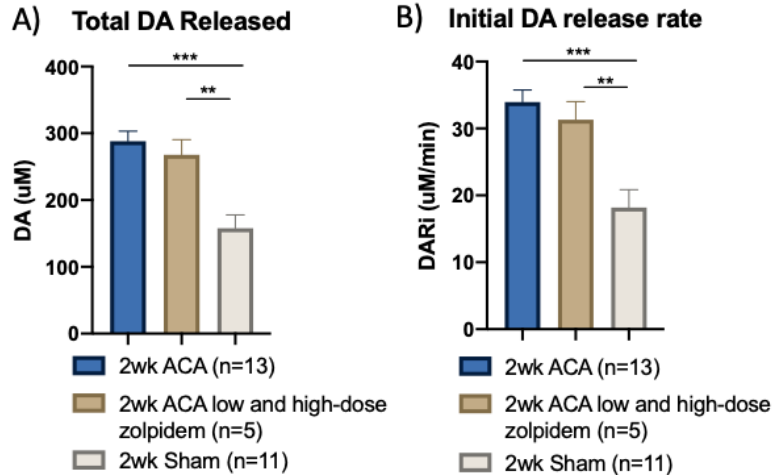


Figure 17: Mean \pm SEM values of total DA released (a) and initial DA release rate (b) in the D-STR following 60Hz,10s stimulation two weeks post-surgery.

(a) ANCOVA showed main effect of group (** $p < 0.0011$), but no main effect of Lactate median or ABE median. Post hoc Tukey's test show significant differences between 2wk ACA and 2wk Sham groups (** $p < 0.0001$), as well as between 2wk ACA zolpidem and 2wk Sham groups (** $p = 0.0017$). (b) ANCOVA showed main effect of group (** $p < 0.0002$), but no main effect of Lactate median or ABE median. Post hoc Tukey's test show significant differences between 2wk ACA and 2wk Sham groups (** $p < 0.0001$), as well as between 2wk ACA zolpidem and 2wk Sham groups (** $p = 0.0025$).

Figure 15 shows group comparisons for DA reuptake-based metrics for untreated ACA, zolpidem-treated ACA, and Sham animals at day 14 post-ACA/Sham surgery. QN simulations revealed that maximal velocity of DA reuptake (V_{max}) from 60 Hz, 10 s stimulations was significantly increased in both untreated and zolpidem-treated ACA groups two weeks post-injury (Fig. 15a) while K_{mi} remained unchanged for both ACA groups compared to Sham animals (Fig. 15b).

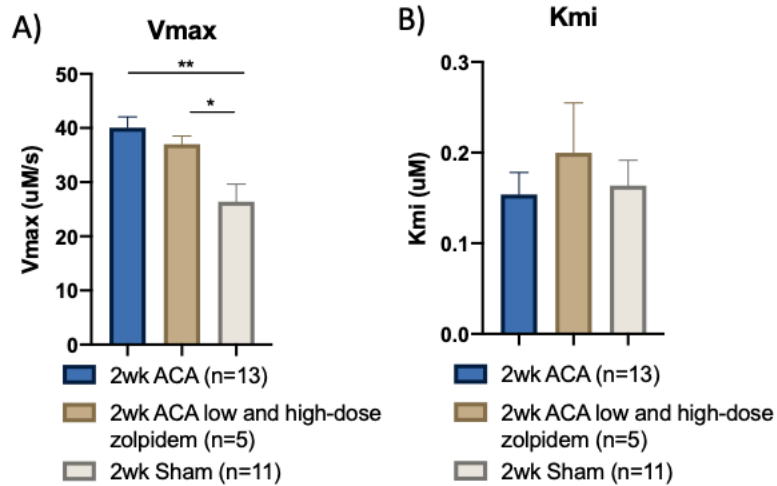


Figure 18: Mean ± SEM maximal DA reuptake velocity (Vmax) (a) and Kmi (b) for each group.

(a) ANOVA showed significant main effect of group ($*p < 0.0001$) for Vmax. Post hoc Tukey's test showed significant differences between 2wk ACA and 2wk Sham groups ($**p = 0.0004$), as well as between 2wk ACA zolpidem and 2wk Sham groups ($*p = 0.0238$). (b) ANCOVA showed no significant differences across groups for Kmi.**

4.0 Regional Zolpidem Microinjections to Reverse HIBI-Induced Striatal Hyperdopaminergia – A Conceptual Experiment

Introduction

HIBI affects certain brain regions more than others. Striatal medium spiny neurons (MSNs), particularly those expressing D2 receptors (D2Rs), are particularly vulnerable to ischemic damage and exhibit early, irreversible damage from ischemia¹⁹. Striatal MSNs also receive dense DAergic input from the substantia nigra pars compacta (SNpc) and evidence shows uncontrolled DA release seen after even a mild hypoxic-ischemic insult, which is more severe than ischemia-induced increases of other neurotransmitters^{27,28}. Through their modulation of cortical, thalamic, and limbic glutamatergic input, as well as spiny striatal acetylcholine (ACh) interneurons, MSNs play key roles in cognition, behavior, motivation, and controlled movement. Aberrant DA signaling underlies various movement disorders, such as in Parkinson's disease (PD) and Huntington's disease (HD)²⁹, suggesting DA neurotransmission changes after CA may facilitate HIBI-induced motor abnormalities. The thalamic reticular nucleus (tRN) is also particularly vulnerable to ischemic injury and animal CA models have demonstrated hyperactive thalamocortical signaling⁷⁰. Another primarily GABAergic region, the tRN provides inhibitory modulation of the intralaminar (iLN) thalamus⁸³, a crucial component of the reticular activating system (RAS) which, through its communication with the cortex, regulates conscious states⁸⁴. HIBI-induced neuronal damage in the tRN likely facilitates abnormal thalamocortical signaling that drives DoC after CA.

Striatal MSNs project topographically to the internal and external globus pallidus (GPi and GPe, respectively) as part of the “direct” and “indirect” pathways of movement, and SNc DAergic

afferents influence these pathways through their effect on different DA receptors. DA exerts an excitatory effect on D1R-expressing MSNs (of the “direct” pathway) and an inhibitory effect on D2R-expressing MSNs (of the “indirect” pathway)⁸⁵. Ascending ACh interneurons modulate these effects by acting as pacemakers, tonically regulating striatal MSN output^{86,87}. DA Striatal MSNs also project to the substantia nigra pars reticulata (SNpr) and SNpc^{88,89}. Striatal DA release by dopaminergic SNpc projections are regulated in part by direct and indirect GABAergic feedback from MSNs^{33–35} and this GABAergic control of the SNc strongly influences its firing properties³⁴. GABAergic afferents from the GPe also strongly influence the firing properties of both nigral regions^{34,36,37}. Disrupted GABAergic outflow resulting from MSN damage or dysfunction may facilitate striatal hyperdopaminergia as well as abnormal thalamocortical transmission that manifests itself as movement and hypo-arousal disorders.

Recent clinical evidence highlights zolpidem, otherwise known as Ambien, as an effective therapy to treat post-HIBI symptoms^{63,65}. Though a well-known hypnotic agent, a growing body of research has studied zolpidem as a tool to promote emergence from DoC, and clinical evidence shows that a short course of zolpidem treatment acutely following HIBI from CA can lead to paradoxical improvements in arousal^{61,63–65}. Zolpidem is a GABA_A receptor agonist with a high selectivity for those expressing the $\alpha 1$ subunit. These receptors, expressed in the striatum, GP, SN, and thalamic nuclei exert a direct influence on striatal DA neurotransmission and thalamocortical signaling⁶⁹. Zolpidem administration has been linked to improvement in Parkinson’s associated movement disorders^{66,67}, possibly by inhibiting GPi-induced thalamocortical hyperactivation and/or other sites where GABA-A receptor inhibition impacts DA transmission directly, such as the SNpr and SNpc⁶⁹. However, the paradoxical response to

zolpidem after brain injury is largely theoretical^{68,90}, and its clinical use has been met with highly mixed results^{72–76}.

The results from our preliminary study detailed in the previous aim also show mixed effects of chronic systemic zolpidem administration on improving outcome after CA. FSCV findings show a modest decrease in evoked striatal DA after chronic zolpidem treatment. High dose zolpidem (0.2mg/kg daily) normalized acoustic startle responses and reversed anhedonia as represented by increased sucrose preference. However, other DA release-based metrics as well as DA clearance/reuptake metrics remained unchanged, and the occurrence of myoclonus and exploratory behavior remained relatively unchanged. Interestingly, the higher dose of zolpidem administered resulted in a dichotomy of outcomes for both myoclonus and open field testing, resembling a group of “responders” and one of “non-responders” with regard to treatment. One explanation is that GABA_A α -1 receptor density varies across the regions where they are localized. For example, they are expressed in higher concentration in the GP compared to the striatum⁹¹. Taken with the GABA_A α -1 receptor’s expression within several basal ganglia regions, systemic zolpidem may exert different downstream effects depending on where it binds these receptors.

Characterizing zolpidem’s effects when localized to particular regions of the striatal-pallidal-thalamocortical circuitry may elucidate the influence these different regions have in mediating HIBI-induced neurological sequelae, as well as assess the efficacy of GABA_A α -1 receptors as a therapeutic target for treating hyperdopaminergia and associated behavioral deficits after ACA. This conceptual study evaluates the presumed impacts of zolpidem microinjections into the GPe in a rat model of asphyxia cardiac arrest (ACA). Given the modest reductions in evoked striatal DA seen in the previous aim and the GPe’s high concentration of GABA_A α -1 receptors, perhaps systemic zolpidem exerted its mildly beneficial effects through this region. As

such, it is hypothesized that intra-pallidal zolpidem may “replace” functions of dysfunctional MSNs and normalize striatal GABAergic outflow to the SNpr and SNpc, thus restoring GABAergic feedback to nigral DAergic neurons and reversing striatal hyperdopaminergia.

Methods

Prior to surgical procedures, rats will be housed in pairs, then housed alone following recovery from the surgeries. Rats will be granted unrestricted access to food and water as well as a 12 h light/dark cycle. Rats will be randomly assigned to one of the following groups outlined in Table 1 below. Microinjections will be performed for groups of n=6 for ACA animals, and n=4 for sham/naïve animals, based on previous studies employing regional zolpidem microinjections^{92,93}. Rats assigned to the ACA or sham group will undergo identical surgical and post-operative procedures as described in prior sections of the thesis.

Table 9: Injury and treatment group counts.

Injury Group	Treatment	Microinjection (GPe)
ACA	Vehicle (DMSO + aCSF)	N=6
Sham	Vehicle (DMSO + aCSF)	N=4
Naive	Vehicle (DMSO + aCSF)	N=4
ACA	Zolpidem	N=6
Sham	Zolpidem	N=4
Naive	Zolpidem	N=4

Fast Scan Cyclic Voltammetry

Two weeks following ACA / Sham procedures, rats will undergo fast scan cyclic voltammetry (FSCV) to measure regional variations of DA neurotransmission based on previously used methods, but with modifications appropriate for this experiment. Experimental DA responses will be obtained using alternating 60- and 40 Hz stimulations for 5- or 10 s according to the schematic depicted in Figure 1. For data analysis purposes, 5- and 10 s recordings at 60 Hz stimulation will be applied prior to any drug or vehicle microinjection. We then applied 60 Hz, 5 s stimulations at 10- and 35 min after vehicle or zolpidem infusion as well as 40 Hz 5 s stimulations at 25- and 50 min after vehicle or zolpidem infusion.

Following *in vivo* electrode measurements, electrodes will be calibrated with seven DA concentrations in artificial cerebrospinal fluid (pH = 7.2) composed of (in mM): 1.2 CaCl₂, 2.0 Na₂HPO₄, 1.0 MgCl₂, 2.7 KCl, and 145 NaCl₈₀. The DA concentration versus current calibration

using a quadratic regression will be used to convert experimental DA responses from measured currents to DA concentrations.

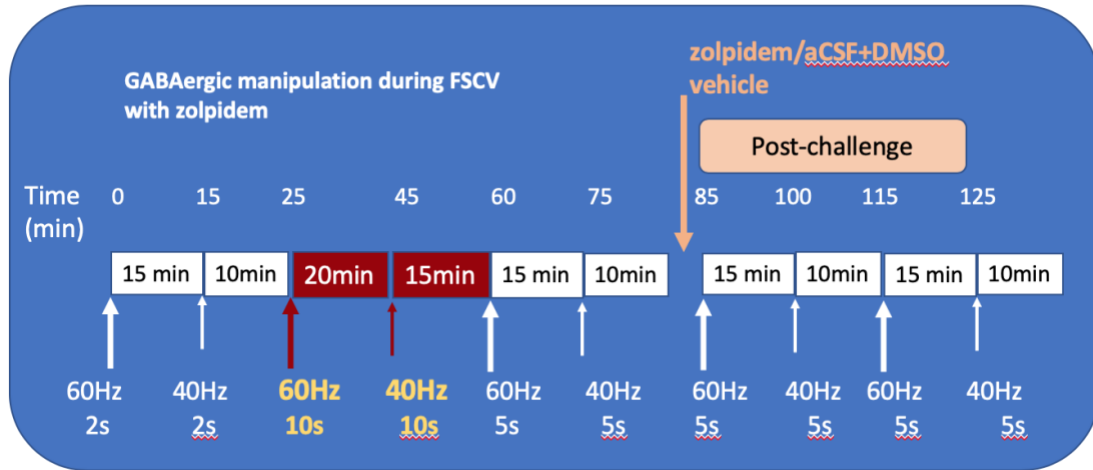


Figure 19: Schematic representation of FSCV experimental study and microinjection timepoints.

Regional Microinjections

While under urethane anesthesia associated with FSCV. Midline incisions will be made, and soft tissues lifted to expose the skull, at which point burr holes will be drilled contralaterally to CFE burr hole for the placement of a microsyringe needle. A craniotomy will be performed at coordinates 1.0-2.0 mm posterior and 3.0-4.0 mm lateral from bregma^{81,94} for needle placement into the GPe.

At the end of baseline FSCV procedures, rats will be implanted with a 32-g stainless steel cannula (Hamilton). A micro-syringe (Hamilton) will be connected through the cannula to an infusion pump (World Precision Instruments) and lowered into the brain. The needle will be lowered to the following coordinates (relative to bregma) for GPe microinjection: AP: -1.4 mm; ML: 3.6mm; DV: -6.6mm⁹⁴. 100nM or 1mM of zolpidem⁹³ dissolved in 2uL vehicle (80% aCSF,

20% DMSO), or 2uL vehicle (aCSF) will be infused into the GPe at a rate of 0.5uL/min. The needle will be left in place for another 3 minutes to ensure compound diffusion.

Verification Of Stereotaxic Coordinates

Following FSCV procedures, regional microinjection sites will be verified using Evans Blue dye. 2uL of Evans Blue dye will be infused into the GPe at a rate of 0.5uL/min and the needle will be left in place for another 2 minutes to ensure compound diffusion before removing the needle, electrodes, and temperature probes.

Rapid decapitation will be performed using a guillotine and the brain will be extracted from the skull using surgical rongeurs before drop-fixing in 10% formalin. After 48 hrs, the brain will be placed in a rat brain slicer matrix (Kent Scientific), and 1mm coronal sections will be cut. Correct infusion location will be verified using a rat brain atlas and regional landmarks as reference such as the striatum's striped appearance or the prominence of the third and lateral ventricles relative in the slices relative to those in the neuroanatomical atlas. Only animals which have had correct infusion locations verified will be added as viable data.

Proposed Results

HIBI results in damage or dysfunction of metabolically vulnerable MSNs, effectively damaging one of the primary sources of inhibition on SNpc DAergic neurons³⁴. To help replace a function of these dysfunctional MSNs, GPe microinfusion of GABA_A α -1 receptor agonist, zolpidem, was proposed. In ACA animals, zolpidem infusion would presumably decrease GPe outflow due to its relatively dense population of GABA_A α -1 receptors. Given the degree of GPe projections to SNpc DAergic neurons^{34,36,95}, this decreased pallidal outflow could potentially exacerbate striatal hyperdopaminergia via their disinhibition. It is hypothesized that lower dosages

of zolpidem in the GPe would elicit this harmful effect. However, the GPe strongly influences the firing properties of both nigral regions^{34,36} and the firing pattern of SNpc DA neurons is largely modulated by SNpr GABAergic neurons³⁷. Further, nigral GABAergic neurons are more sensitive to GABA_A-mediated inhibition than nigral dopaminergic neurons, in part due to a more hyperpolarized GABA_A reversal potential³⁷. Therefore, decreasing pallidal inhibitory drive should disinhibit these SNpr GABAergic neurons, and consequently increase their inhibitory drive onto DAergic SNpc neurons, thus reversing post-HIBI striatal hyperdopaminergia. It is expected that this effect would result from larger doses of intra-GPe zolpidem.

In terms of the voltammetric signals obtained from the FSCV experiment, inhibition of SNpc DAergic neurons would be represented as reduced amplitude and concentration of evoked DA, as well as a reduction in the initial DA release rate. With regard to DA clearance and reuptake, an acute drug challenge may not be evident via reduced velocity of DA reuptake (V_{max}). 5-min VF-CA animal models show a considerable upregulation of striatal DA transporter (DAT) as well via western blot analysis. Concurrently, western blot analysis of experimental TBI models, which suggest a functional *hypo*-dopaminergia, show a corresponding *decrease* in V_{max} and striatal DAT expression, suggesting that chronic changes in V_{max} may occur as a compensatory mechanism to combat aberrant DA neurotransmission. Sham and Naïve animals would presumably react differently to intra-GPe zolpidem because they still retain normal striatal GABAergic outflow. Further inhibiting the GPe may result in a suppression of striatal DAergic tone due to disinhibition of SNpr GABAergic neurons, and the corresponding voltammetric readouts in these animals may resemble the diminished DA neurotransmission observed in experimental TBI models. However, zolpidem in the GPe will inhibit a combination of SNpr neurons and SNpc DAergic neurons. At smaller doses, zolpidem may exert minimal effects on

striatal DA neurotransmission due to its mixed actions on SNpr and SNpc neurons combined with the striatal MSN inhibitory drive on SNpc DAergic neuron firing. For any injury group, vehicle injections should exert minimal effects on voltammetric DA responses compared to animals not receiving any microinjections, and resemble similar responses observed for 5min- ACA, Sham, or Naïve animals⁶.

Discussion

This study evaluated the proposed effects of GABAergic modulation of the GPe, via zolpidem microinfusion, to reverse striatal hyperdopaminergia stemming from a 5-min ACA. It is hypothesized that larger doses of intra-GPe zolpidem will help reverse striatal hyperdopaminergia by disinhibiting SNpr GABAergic neurons thus indirectly inhibiting SNpc DAergic neuronal firing, as described in figure 20.

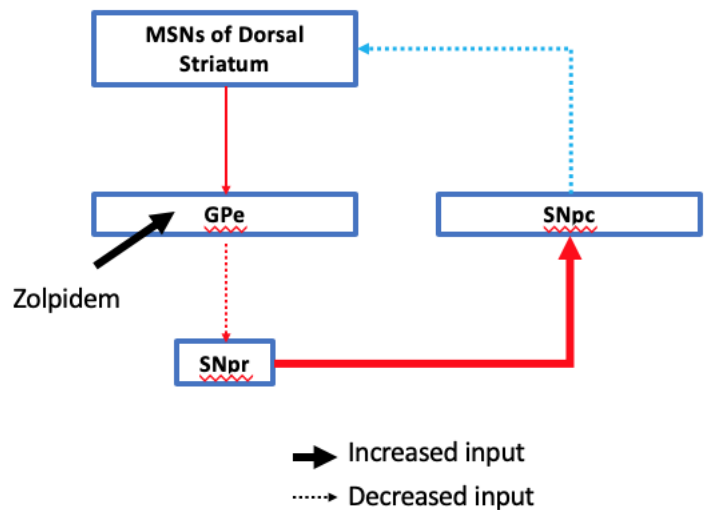


Figure 20: Proposed effects of intra-pallidal zolpidem

Zolpidem microinjections into the GPe may disinhibit SNpr GABAergic neurons, thus re-introducing inhibitory drive onto SNpc DAergic neurons and reversing striatal hyperdopaminergia.

However, these DAergic neurons receive afferent input from other regions which complicate the effects of GPe modulation on SNpc neuronal firing. The subthalamic nucleus (STN), another main output target of the GPe and a primarily glutamatergic region, may play a role in regulating DAergic neuron firing through NMDA receptor stimulation⁹⁶⁻⁹⁸. GPe inhibition will disinhibit the STN which may counteract the previously proposed effects of intra-GPe zolpidem on DAergic neuron firing.

HIBI's long-term effects on the basal ganglia circuitry should also be considered. In addition to striatal, pallidal, and thalamic neuron damage/dysfunction, ischemic injury also delayed damage to SNr GABAergic neurons as early as three weeks following injury⁹⁹. As these neurons are the primary source of inhibition on nigral DAergic neurons, delayed SNr damage post-HIBI likely exacerbates SNc disinhibition after the injury. However, SNpr damage might allow other SNpc afferents to exert more influence over DAergic neuron firing, such as the smaller population of SNpc GABAergic neurons.

In addition to striatal hyperdopaminergia that likely underlies post-HIBI motor impairments, CA survivors commonly suffer from DoC likely due to abnormal thalamocortical signaling mediated by tRN damage. The tRN also has a very dense GABA_A α -1 receptor population even compared to the GP₉₁, further suggesting the idea that systemic zolpidem administration affects several different regions and at different capacities, which may explain the mixed effects of systemic zolpidem observed in animal models and clinical studies.

Future work should evaluate the effects of intra-thalamic zolpidem injections as they may help replace the function of damaged tRN GABAergic neurons after CA. Rather than FSCV, these studies could utilize electrophysiology techniques to evaluate changes in thalamocortical neuronal firing after intra-thalamic zolpidem administration. Additional work should continue exploring the

differential effects of systemic zolpidem administration vs. microinfusions at varied post-HIBI timepoints, and this can be done in concert with neuronal tissue staining and western blot analyses to further characterize the time-course of neuronal damage and protein expression changes that mediate HIBI-relevant symptomologies. Though microinfusions pose practical obstacles for treating clinical populations, their use may offer key mechanistic insights to HIBI-induced neuronal dysregulation brought that drives motor and cognitive impairments, thus highlighting other therapeutic targets for treating CA survivors.

5.0 Discussion

Cardiac arrest produces global cerebral ischemia that commonly results in HIBI among survivors. Though limited, the use of acute neurological and physiological readouts suggests promise as prognostic tools for ischemic injuries, so we evaluated their utility in predicting long-term behavioral outcomes. HIBI results in disruptions DA neurotransmission, which under physiologic conditions, mediate motor, cognitive, and behavioral functions. As such, how these injury severity readouts align with electrically stimulated DA neurotransmission outcomes was also explored.

These results show that a neurological readout, as defined by the neurological deficit score, is a valuable predictor of survival after a 5-min ACA. When comparing values between survivors and non-survivors, only NDS showed a significant difference of the three metrics evaluated, suggesting that acute mortality after the ACA is likely due to neurological injury rather than cardiovascular injury. The Cox regression showed increases in NDS increase the hazard ratio of protocol exclusion either by death or severe distress by almost 40%. NDS, lactate, and ABE covariate data from the Cox regression were also used to predict survival probabilities up to a week post-injury. Even as estimated values, these prediction data may prove useful to pre-clinical technicians for honing experimental CA models. Acute NDS was also significantly correlated with day 14 post-injury NDS, further suggesting their utility in predicting long-term neurological outcome after ACA.

Spearman's rank correlations showed associations between DA release-based metrics and lactate, and ABE, respectively, suggesting that these physiological readouts may align with ACA-induced deficits at a more granular level than NDS. Though ABE serves as a prognostic tool in a

clinical setting, the experimental ACA surgery procedure may influence these data. For example, intravenous bicarbonate is administered to promote return-of-spontaneous-circulation (ROSC) by directly combating acidosis caused by the cardiac arrest. As ABE is an inverse measure of acidosis, this resuscitation tool likely influences acute ABE values.

Because DA neurotransmission abnormalities are likely related to commonly observed cognitive and behavioral impairments after HIBI, partial correlation analyses were employed to identify functional coupling between them before and after adjusting for NDS, lactate values, and ABE values. The 85-dB and 95-dB sound bursts in the ASR assessment positively correlated with evoked DA at 1s (into electrical stimulation). Sucrose preference inversely correlated with maximal evoked DA as well, suggesting a functional coupling between DA release-based metrics and behavior, in addition to physiological readouts. Further, adjusting for ABE as a covariate attenuated the associations between ASR metrics and evoked DA at 1s, while strengthening the inverse association between sucrose preference and maximal evoked DA. As described above, however, the influence ABE exerts over these long-term associations should be considered as a potential confound in an experimental CA setting.

The neurological injury induced by circulatory arrest determines a patient's prognosis after CA, and these injury-induced changes in cerebral blood flow (CBF) affect neuronal bioenergetics and result in neuronal damage/dysfunction that may drive DA neurotransmission and behavioral abnormalities. Post-CA CBF properties also change over time which may drive neuronal damage and dysfunction¹⁰⁰. Cerebral perfusion after resuscitation is characterized by early hyperemia followed by hypoperfusion and, ultimately, restoration of normal blood flow approximately 72 hrs following resuscitation¹⁰⁰. At the level of microcirculation, CBF is heterogeneous and characterized by areas of no flow, low flow, and increased flow in certain brain regions¹⁰¹, such as

the “no flow phenomenon” observed, via animal models, in cortical capillaries¹⁰¹. CBF directed therapies tested in animal CA models, such as the use of albumin¹⁰², have improved neurological outcome, suggesting that post-CA CBF alterations contribute to the development of HIBI. However, little work has been done in the clinical population for utilizing CBF directed therapies to improve neurological outcome after CA¹⁰¹. Although the present study focused on the two-week post-injury timepoint, preliminary data from our lab (not shown) shows dynamic changes in DA neurotransmission over time following HIBI. The energy deficiency caused by HIBI leads to a breakdown in neuronal concentration gradients, allowing for calcium influx that drives mitochondrial damage and cell death¹⁰³. Bioenergetic changes following HIBI may alter MSN activity as well, leading to dynamic changes in DA neurotransmission over time. In the acute post-injury phase, The HIBI-induced blood flow disruptions deprive MSNs of their energy reserves quickly due to their high metabolic demands, eliciting a rapid dissolution of their electrochemical gradients and cell depolarization¹⁰⁴. The resulting high MSN activity drives inhibition to MSN target regions including the GP and the SNpc, the latter of which may inhibit DA neurotransmission and lower striatal DA levels. As these brain regions slowly recover from the initial injury, compensatory changes may continue to drive DA neurotransmission changes and dynamic neuronal dysfunction. Future research should verify the rate at which HIBI depletes MSN energy reserves and how MSN depolarization impacts DA release. Further, research should characterize MSN bioenergetic properties over time to elucidate their changes and how they may impact striatal DA neurotransmission over time.

The neurobiological mechanisms underlying depression are not well understood. Depression symptoms like anhedonia implicate a number of highly interconnected brain regions, making it difficult for clinicians and researchers to elucidate its molecular mechanisms¹⁰⁵. HIBI

disrupts multiple brain areas directly and indirectly implicated in depression. Researchers highlight the potential role of striatal DA aberrations as a potential mediator of depression symptoms. Early hypotheses have suggested a link between DA deficiency and depression because past research showed beneficial effects of dopamine precursors and agonists on ameliorating depressive symptoms¹⁰⁶. The effects of experimental TBI generally align with this hypothesis, as TBI induces a suppression of striatal DA neurotransmission⁵, and post-TBI depression is well documented in clinical practice. However, the results at hand show a robust state of striatal hyperdopaminergia as well as anhedonia after a 5-min ACA. Additionally, the large inverse correlation between sucrose preference and maximal evoked DA derived from partial correlation analyses suggests that anhedonia increases in severity as striatal DA increases.

A large body of animal research focuses on the hippocampus and frontal cortical regions as key mediators of depression¹⁰⁷, both of which are selectively vulnerable to HIBI. There is some evidence of reduced hippocampal volumes in depressed or PTSD patients¹⁰⁸. As the hippocampus exerts inhibitory control over the hypothalamic-pituitary-adrenal (HPA) axis, a decline in hippocampal function may contribute to hypercortisolemia observed in a population of depressed patients^{109,110}. One study used positron emission tomography to identify abnormal hippocampal and cortical blood flow in depressed individuals¹¹¹. The thalamus may also contribute to post-HIBI depression. Neuronal damage in the thalamic reticular nucleus (tRN), brought on by global ischemia, leads to elevated firing rates of thalamocortical neurons⁷⁰, and impaired thalamocortical connectivity with the prefrontal and anterior cingulate cortices (aCC) facilitates disorders of consciousness¹¹². Considering the aCC's role in emotion processing, morality, impulse control, and other limbic behaviors, altered thalamocortical signaling after HIBI may mediate depression symptoms.

In addition to mechanical damage and neuronal dysfunction, brain injuries also elicit severe inflammatory responses which potentially drive a number of symptoms. Sickness behaviors refer to behavioral changes that result from central neural activity changes. These behaviors are often encountered during acute systemic infections and are an important adaptive survival mechanism¹¹³. Depression is among the most common symptoms accompanying traumatic brain injuries^{114,115}. The high incidence of sickness behaviors with systemic inflammatory diseases occurring outside the CNS suggests that their association with these ischemic brain injuries is in part driven by inflammation. With HIBI and its effects on basal ganglia circuitry, inflammation can strongly impact multiple parameters associated with striatal DA neurotransmission and affect functional connectivity between brain regions that behaviors including motor activity, depression, and anxiety^{43,44,116}. Experimental models of ventricular fibrillation cardiac arrest (VF-CA) demonstrate persistent striatal Iba staining⁴⁶, suggesting striatal microglial activation in response to VF-CA. Robust increases in tumor necrosis factor-alpha (TNF α) are also seen in the striatum after VF-CA^{46,117}. Taken with the minimal changes in striatal protein expression observed after VF-CA⁶, one hypothesis for hyperdopaminergia and the associated anhedonia/depression is ongoing neuroinflammation.

The acoustic startle circuit is a reflexive, tri-synaptic pathway primarily localized to the pons and the spinal cord^{53,118}. Auditory information is translated into neural signals at the cochlear nuclei. The cochlear nuclei then relay these signals via the 8th cranial nerve to the pontine reticular nucleus (PnC), a key contributor to sensorimotor integration and plasticity of the acoustic startle reflex (ASR)^{51,52}. PnC projections innervate hundreds of motor neurons, via the reticulospinal tract in the medial longitudinal fasciculus of the spinal cord, in response to the stimulus.

However, ASR disruptions are associated with neurological disorders like TBI and schizophrenia, which are not directly involved with this primary circuitry, and implicate aberrant DA signaling in these secondary brain regions. TBI induces long-lasting ASR suppression without prompting degeneration of its essential neural circuit⁴⁷. TBI does induce hippocampal and cortical cell death, however, suggesting that a primary cortical impact can influence brainstem circuit function. Additionally, striatal DA neurotransmission suppression associated with experimental TBI models corroborates the idea that dopaminergic signaling directly influences the ASR.

Other neurological disorders such as schizophrenia are characterized by overactive DA systems and dysregulated cortical-striatal circuitry and result in ASR hypersensitivity and PPI deficits^{48,49}. Our study demonstrated that a 5-min ACA results in ASR hypersensitivity and PPI deficits three days following the injury, and that ASR metrics correlated with evoked DA metrics, corroborating this positive relationship between ASR and DA signaling. HIBI results in damage/dysfunction of metabolically vulnerable MSNs, particularly those expressing D2Rs, likely reducing striatal GABAergic outflow. In turn, the globus pallidus loses a main source of inhibitory input, and the resulting increase in pallidal outflow indirectly disinhibits SNpc DAergic neurons. Recent studies utilizing tract tracing methods demonstrate that the SNpc directly exerts dopaminergic tone on the PnC¹¹⁹ in addition to its striatal and cortical projections, offering a potential mechanistic link for amplified ASR after ACA-induced HIBI.

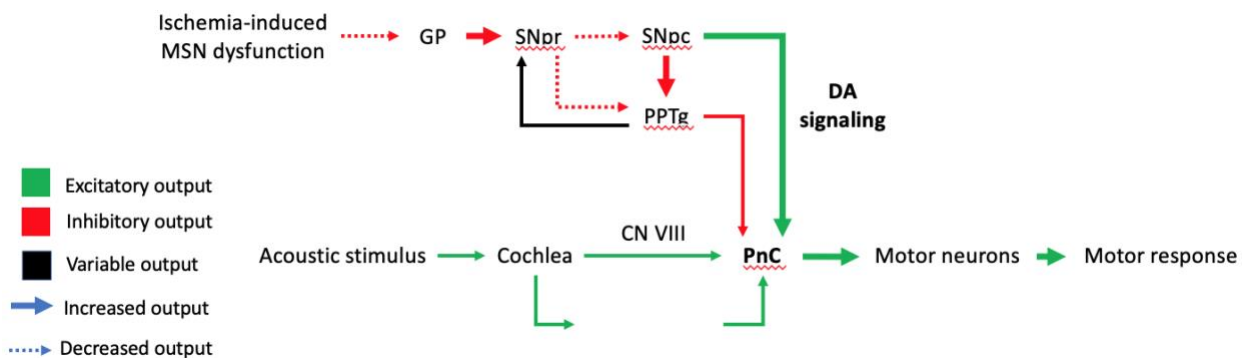


Figure 21: Schematic of acoustic startle response pathway influenced by HIBI

Ischemia-induced MSN dysfunction disinhibits the GP and indirectly leads to increased firing of SNpc DAergic neurons. Because the SNpc directly innervates the PnC, a key region for mediating the acoustic startle response, HIBI may result in amplified acoustic startle responses due to increased SNpc outflow.

Myoclonus refers to sudden, involuntary muscle jerks, shakes or spasms, and these abnormal involuntary movements are a hallmark feature of post-HIBI symptomologies.

Mechanisms underlying post-hypoxic myoclonus (PHM) are not well understood but thought to arise due to neuronal hyperactivity following the ischemic brain injury¹²⁰⁻¹²². As such, anticholinergic and anticholinergic agents have been tested with some success to attenuate PHM in animal CA models, and to promote neuroprotection of hippocampal and cerebellar neurons^{123,124}. Piracetam is a GABA derivative but through its modulatory actions on a range of neurotransmitter systems including cholinergic and glutamatergic, exerts robust anti-myoclonic effects in animal CA models and in humans^{124,125}. Though multiple therapeutic agents tested have successfully attenuated PHM, the neurobiological mechanisms underlying PHM and audiogenic seizures remain poorly understood. One explanation for PHM is cerebellar damage, particularly the purkinje neurons, following ischemic brain injury. Basal ganglia circuits were considered to be anatomically and functionally distinct from cerebellar circuits¹²⁶, but a number of subsequent

studies challenge this perspective. A disynaptic projection between the cerebellar dentate nucleus and dorsal striatum have been described using retrograde transneuronal transport methods¹²⁷. Another study links the cerebellar cortex and subthalamic nucleus¹²⁸. This work utilizing tract tracing methods provides evidence for substantial communication between the cerebellum and basal ganglia that is independent of the cerebral cortex¹²⁸.

This study shows robust occurrences of myoclonic responses two days following ACA, and other data (not shown) from our group shows that myoclonus persists at least twelve days following ACA. Future research should utilize fluorojade staining to evaluate if cerebellar cell death correlates to occurrence of myoclonic responses, which may provide clues for the source of this phenotype after HIBI.

Given the impact of ACA-induced HIBI on striatal MSNs as well as the larger associated basal ganglia circuitry, we evaluated the effects of chronic, systemic zolpidem administration on normalizing striatal DA neurotransmission and ameliorating HIBI-induced behavioral deficits.

Maximal evoked DA were not significantly different between zolpidem-treated and untreated ACA animals. However, ANOVA showed that zolpidem-treated (0.1mg/kg and 0.2mg/kg) animals were not significantly different from Sham animals either, suggesting a very modest reduction in maximal evoked DA compared to the untreated ACA group. Further, daily zolpidem had no apparent effect on DA release or DA reuptake kinetics, with outcomes remaining significantly different from sham animals for total DA released, initial DA release rate, and V_{max}. With regard to reflexive behavior, the higher zolpidem dose (0.2mg/kg) normalized ASR outcomes for the 95-dB and 105-dB sound bursts but had minimal effect on reducing occurrence of myoclonic responses 2 days post-injury. High dose zolpidem also had mild beneficial reductions in anhedonia compared to untreated ACA animals. Similar to myoclonic responses, neither the

pooled group of low-and high-dose zolpidem-treated animals nor the high dose zolpidem group on its own significantly improved exploration or mobility in the open field.

Interestingly, the high dose zolpidem groups showed a dichotomy of outcome for both dosages, broken up into “responders” and non-responders”. The lack of significant zolpidem effects on behavior and DA neurotransmission could be due to the small sample size, but the basal ganglia’s dispersed distribution of GABA-A receptors and dynamic changes in neuronal damage/dysfunction resulting from HIBI greatly complicate the effects of systemic zolpidem administration. GABA_A α -1 receptors are the principal target of zolpidem. the α -1 subunit is the most abundant GABA_A subunit and is found with variable distribution throughout the brain 1,2. Within the structures of interest, GABA_A α -1 receptors are found in low concentrations in the striatum and SN, high concentrations in the GP, and very high concentrations in various thalamic nuclei including the tRN₉₁. SNpr GABA-A receptors mediate nigral GABAergic output, but these receptors are also found on DAergic SNpc neurons where their activation causes DA neuron inhibition. In fact, 70% or more of SNpc DAergic neuron afferents are GABAergic³⁷, and are largely projected from the SNpr.

Neither low- or high-dose zolpidem significantly reduced evoked DA. Considering the spatial distribution of GABA_A α -1 receptors throughout the basal ganglia, systemic zolpidem administration may selectively bind pallidal GABA_A α -1 receptors, thus increasing pallidal output. Whereas inhibition of pallidal output on the part of zolpidem presumably leads to a decrease in the firing of DA neurons due to disinhibition of SNpr GABAergic neurons, an increase in pallidal output may lead to burst firing in DA neurons and a significant increase in extracellular striatal DA³⁷, despite its expected inhibitory effects on dopaminergic neuron firing. Nigral GABAergic neurons are more sensitive to GABA_A-mediated inhibition than nigral dopaminergic neurons, in

part due to a more hyperpolarized GABA-A reversal potential³⁷. This effect is so robust that the systemic administration of the GABA-A agonist, muscimol, leads to an increase in spontaneous DA neuron firing rates¹³⁰ and elicits an increase in striatal dopamine levels^{131,132}. Low-intensity electrical stimulation of these GABAergic afferents³³ also prompts activation and asynchronous GABA release, preferentially inhibiting the more sensitive GABAergic neurons with only minimal direct effects on the dopaminergic neurons. This leads to a disinhibition of the dopaminergic neurons as the tonically active SNpr GABAergic neurons are silenced, resulting in an increase in burst firing and a consequent increase in striatal dopamine levels despite only a minimal increase in their firing rate³⁵. Although all of these manipulations likely add some direct inhibition of nigral dopaminergic neurons, they remove a far greater amount by inhibiting the tonically active SNpr GABAergic neurons. Given the dichotomy in behavioral outcomes observed with the high dose zolpidem group, higher zolpidem concentrations may mediate this SNpc disinhibition that exacerbates striatal hyperdopaminergia. Future work should assess DA neurotransmission in ACA animals given higher doses of zolpidem in order to elucidate the effects of higher zolpidem concentrations on striatal DA levels.

Regional differences within the dorsal striatum relative to electrode placement during FSCV studies may have also impacted varied DA responses. The dorsal striatum is also a functionally heterogeneous region, with microstructure differences in the grey and white matter (a.k.a. striata) as well as neurochemically distinct striosome and matrix compartments, and these distinct compartments exhibit differing DA release properties^{133,134}. Though our FSCV studies employed consistent coordinates for carbon fiber electrode placement, heterogeneity from animal to animal may have led to variations of electrode placement relative to different striatal compartments, thus affecting FSCV data readouts. Future work should also contextualize this

heterogeneity in DA neurotransmission relative to ACA to further characterize HIBI-induced DA neurotransmission deficits in the D-STR.

The opposing action of DA and ACh also plays an important role in basal ganglia physiology. MSN output is modulated by striatal aspiny cholinergic interneurons and DAergic stimulation of MSNs is modulated by cholinergic input from aspiny neurons and from glutamatergic cortico-striatal afferents. These are tonically active, pacemaker neurons that in turn receive inhibitory dopaminergic projections from the SNpc^{86,135}, forming a dynamic equilibrium which, when disrupted, drives severe behavioral deficits^{136,137} and movement disorders resembling those associated with PD and HD. PD patients experience a pathologic gain of aspiny ACh output, perhaps consequently from reduced nigrostriatal dopaminergic tone^{135,138}, whereas HD is characterized by a relative loss in striatal ACh signaling that may contribute to movement disorders^{86,138}. The relative overabundance of striatal DA seen after HIBI likely causes tonic inhibition of striatal cholinergic interneurons which, combined with the loss of aspiny ACh output due to MSN damage after HIBI, drive motor abnormalities and DoC that impair function after CA. Aspiny ACh interneurons exert their effect by acting on MSN muscarinic receptors. M4 activation on D1 MSNs blunt MSN output while M1 activation on both D1 and D2 MSNs provides an excitatory effect^{86,139}. M5 receptors also regulate DA release by mediating its release in the SNpc whereas they inhibit DA release from terminals in the striatum¹⁴⁰.

Donepezil, an acetylcholinesterase inhibitor widely used in Alzheimer's and dementia spectrum disorders, has the potential to modulate cholinergic and dopaminergic pathways in the basal ganglia, suggesting promise for its use to modulate post-HIBI movement disorders. Recent studies in mice have demonstrated improved hyper-dopaminergic striatal function with administration of donepezil, effectively elevating acetylcholine levels in the striatum and

counteracting dopaminergic-driven inhibition⁸⁷. Recent clinical case studies report improved arousal and ameliorated motor impairments with a combined administration of donepezil and zolpidem⁶³. The addition of cholinergic modulation (via donepezil) combined with zolpidem may synergistically counter striatal aspiny ACh interneuron inhibition that drives DA signaling disruptions and motor disorders, as well as normalize thalamocortical signaling to rectify DoC post-HIBI. This dual therapy approach may help each individual treatment work more effectively while also limiting their potentially deleterious effects on this ACA-relevant circuitry. Donepezil administration may help reverse striatal hyperdopaminergia by normalizing general MSN firing and the D1 MSN vs. D2 MSN firing mismatch associated with the D2 MSN selective vulnerability to HIBI. Increasing D2 MSN firing will in turn reduce GPe output, which indirectly drives inhibition onto SNpc DAergic neurons. Further, because over-activation of D1 MSNs elevates thalamocortical signaling, donepezil may help to ameliorate post-HIBI DoC by reducing D1 MSN firing.

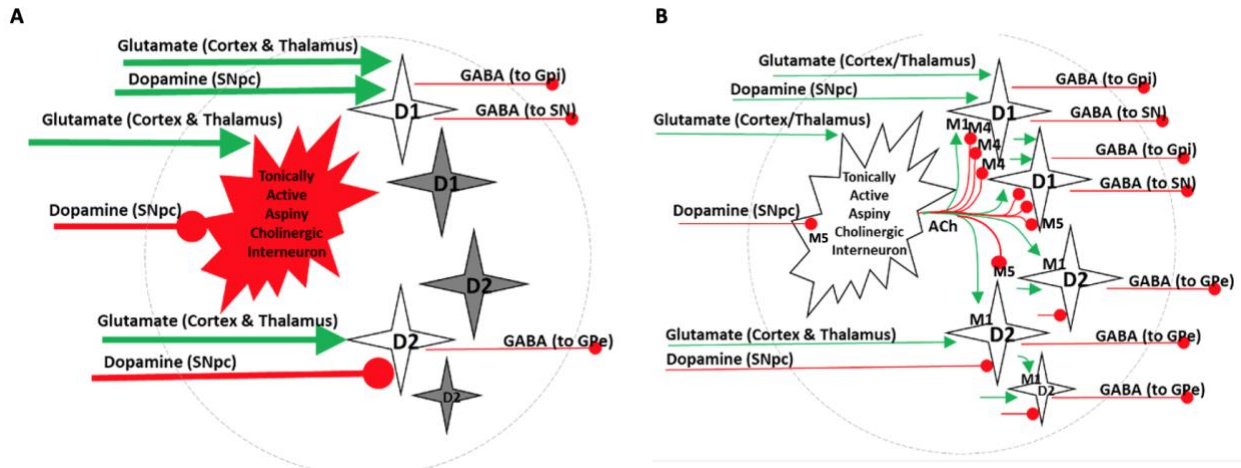


Figure 22: Effects of HIBI on basal ganglia circuitry before (A) and after (B) systemic donepezil administration.

(A) HIBI causes damage/dysfunction to striatal MSNs, particularly those expressing D2Rs. This mismatch is aggravated by striatal hyperdopaminergia, which chronically inhibits aspiny ACh interneurons, thus over-activating D1 MSNs and over-inhibiting D2 MSNs

(B) Donepezil may reverse striatal hyperdopaminergia by reducing D1 MSN firing and increasing D2 MSN firing through increased cholinergic effects on M4 and M1 muscarinic receptors, respectively. Donepezil may reduce DA levels in the setting of hyperdopaminergia directly by M5 effects at DA terminals to decrease DA release.

Though HIBI results in amplified GPi inhibitory drive which would presumably suppress thalamocortical signaling, animal models show elevated thalamocortical neuronal firing after CA_{70,71}. The dense population of thalamic GABA_A- α -1 receptors suggests systemic zolpidem may dominantly exert its effects in the thalamus, helping to normalize thalamocortical signaling as well. Combined with the increased D2 MSN firing due to donepezil treatment, zolpidem may also help to reverse striatal hyperdopaminergia by reducing GPe outflow, indirectly driving inhibition onto SNpc DAergic neurons.

Zolpidem's use as a clinical tool to promote arousal and ameliorate motor impairments in the chronic post-cardiac arrest phase has very mixed results^{66-68,73-76,141}. For individuals who

respond positively to zolpidem in clinical settings, the benefit varies greatly but is generally characterized by short-term improvements in arousal closely associated with the timing of its administration^{66,74,76}. The present study employed lower dosages of zolpidem (0.1-0.2mg/kg) and an administration timepoint relative to subsequent behavioral assessments (20 minutes prior) based on previous animal work, which optimized zolpidem dosages for improving motor deficits in a 6-OHDA lesion study, a common Parkinson's disease model. Future work should further titrate zolpidem administration dosages and timepoints that most effectively combat post-HIBI neurological sequelae.

6.0 Conclusion

This study evaluated the utility of neurological assessments and physiological readouts, in the acute post-ACA phase, for predicting survival probability as well as long-term behavioral and DA neurotransmission outcomes. The Cox regression model ran suggests promise for NDS as a useful prognostic tool. Additionally, the partial correlation analyses employed revealed robust correlations between DA release-based metrics and reflexive and cognitive behavioral outcomes. Our zolpidem pilot study showed mixed effects in its systemic administration improving behavioral impairments and reversing striatal hyperdopaminergia, though the higher dosage evaluated reversed the amplified startle response seen after CA as well as post-CA anhedonia, as defined by ASR and sucrose preference testing, respectively.

Future research should continue exploring the utility of different neurological assessments and acute physiological readouts in predicting long-term survival or behavioral outcomes after ACA. Zolpidem's effects at various dosages and various administration timepoints relative to behavioral assessments, as well as the empirical effects of zolpidem microinjections in different basal ganglia regions should also be explored in addition to the effects of combined cholinergic and GABAergic manipulations with donepezil and zolpidem, respectively. With regard to FSCV, future work should also further characterize heterogeneity of DA neurotransmission properties among different strisomes and striatal matrix compartments by systematically changing measurement coordinates combined with voltammetric and/or electrophysiological recordings. The electrode placements can be histologically verified by identifying capillary tube damage in the striatum and where it is seen relative to the internal capsule or other anatomical landmarks. Additionally, CA research should continue working to unravel the mechanisms underlying HIBI-

induced behavioral impairments with western blotting to evaluate protein expression changes after CA, as well as immunostaining techniques to characterize dynamic changes of microglial/astrocytic activation and inflammatory marker expression that may mediate aberrant DA signaling and post-CA functional impairments. Lastly, the dynamic changes in bioenergetics after CA and how these changes affect neuronal dysfunction in the larger striatal-pallidal-thalamic circuitry should be explored, such as dynamic changes in cerebral blood flow over time – these insights may help to explain dynamic changes in DA neurotransmission or behavioral abnormalities observed at various timepoints following CA.

Bibliography

1. Mozaffarian D, Benjamin EJ, Go AS, et al. Heart Disease and Stroke Statistics—2016 Update. *Circulation*. Published online January 1, 2015:CIR.0000000000000350. doi:10.1161/CIR.0000000000000350
2. Multi-Society Task Force on PVS. Medical aspects of the persistent vegetative state (1). *N Engl J Med*. 1994;330(21):1499-1508. doi:10.1056/NEJM199405263302107
3. Howell K, Grill E, Klein A-M, Straube A, Bender A. Rehabilitation outcome of anoxic-ischaemic encephalopathy survivors with prolonged disorders of consciousness. *Resuscitation*. 2013;84(10):1409-1415. doi:10.1016/j.resuscitation.2013.05.015
4. Lu-Emerson C, Khot S. Neurological sequelae of hypoxic-ischemic brain injury. *NeuroRehabilitation*. 2010;26(1):35-45. doi:10.3233/NRE-2010-0534
5. Bales JW, Wagner AK, Kline AE, Dixon CE. Persistent cognitive dysfunction after traumatic brain injury: A dopamine hypothesis. *Neurosci Biobehav Rev*. 2009;33(7):981-1003. doi:10.1016/j.neubiorev.2009.03.011
6. Nora GJ, Harun R, Fine DF, et al. Ventricular fibrillation cardiac arrest produces a chronic striatal hyperdopaminergic state that is worsened by methylphenidate treatment. *J Neurochem*. 2017;142(2):305-322. doi:10.1111/jnc.14058
7. Drabek T, Foley LM, Janata A, et al. Global and regional differences in cerebral blood flow after asphyxial versus ventricular fibrillation cardiac arrest in rats using ASL-MRI. *Resuscitation*. 2014;85(7):964-971. doi:10.1016/j.resuscitation.2014.03.314
8. Tsai M-S, Huang C-H, Tsai S-H, et al. The difference in myocardial injuries and mitochondrial damages between asphyxial and ventricular fibrillation cardiac arrests. *Am J Emerg Med*. 2012;30(8):1540-1548. doi:10.1016/j.ajem.2012.01.001
9. Laptok AR, Corbett RJT. The effects of temperature on hypoxic-ischemic brain injury. *Clin Perinatol*. 2002;29(4):623-649, vi. doi:10.1016/s0095-5108(02)00057-x
10. Chu Stacy Y., Cox Margueritte, Fonarow Gregg C., et al. Temperature and Precipitation Associate With Ischemic Stroke Outcomes in the United States. *Journal of the American Heart Association*. 2018;7(22):e010020. doi:10.1161/JAHA.118.010020
11. Nikolova S, Lee T-Y, Bartha R. The Severity of Ischemia Varies in Sprague-Dawley Rats from Different Vendors. *ISRN Stroke*. doi:https://doi.org/10.1155/2014/919652

12. Jia X, Koenig MA, Nickl R, Zhen G, Thakor NV, Geocadin RG. Early electrophysiologic markers predict functional outcome associated with temperature manipulation after cardiac arrest in rats. *Crit Care Med*. 2008;36(6):1909-1916. doi:10.1097/CCM.0b013e3181760eb5
13. Neumar RW, Bircher NG, Sim KM, et al. Epinephrine and sodium bicarbonate during CPR following asphyxial cardiac arrest in rats. *Resuscitation*. 1995;29(3):249-263. doi:10.1016/0300-9572(94)00827-3
14. von Auenmueller KI, Christ M, Sasko BM, Trappe H-J. The Value of Arterial Blood Gas Parameters for Prediction of Mortality in Survivors of Out-of-hospital Cardiac Arrest. *J Emerg Trauma Shock*. 2017;10(3):134-139. doi:10.4103/JETS.JETS_146_16
15. Björklund E, Lindberg E, Rundgren M, Cronberg T, Friberg H, Englund E. Ischaemic brain damage after cardiac arrest and induced hypothermia--a systematic description of selective eosinophilic neuronal death. A neuropathologic study of 23 patients. *Resuscitation*. 2014;85(4):527-532. doi:10.1016/j.resuscitation.2013.11.022
16. Brisson CD, Hsieh Y-T, Kim D, Jin AY, Andrew RD. Brainstem neurons survive the identical ischemic stress that kills higher neurons: insight to the persistent vegetative state. *PLoS ONE*. 2014;9(5):e96585. doi:10.1371/journal.pone.0096585
17. Galvin KA, Oorschot DE. Continuous low-dose treatment with brain-derived neurotrophic factor or neurotrophin-3 protects striatal medium spiny neurons from mild neonatal hypoxia/ischemia: a stereological study. *Neuroscience*. 2003;118(4):1023-1032.
18. Wu X, Drabek T, Kochanek PM, et al. Induction of profound hypothermia for emergency preservation and resuscitation allows intact survival after cardiac arrest resulting from prolonged lethal hemorrhage and trauma in dogs. *Circulation*. 2006;113(16):1974-1982. doi:10.1161/CIRCULATIONAHA.105.587204
19. Pulsinelli WA, Brierley JB, Plum F. Temporal profile of neuronal damage in a model of transient forebrain ischemia. *Ann Neurol*. 1982;11(5):491-498. doi:10.1002/ana.410110509
20. Charvin D, Vanhoutte P, Pages C, Borrelli E, Caboche J. Unraveling a role for dopamine in Huntington's disease: The dual role of reactive oxygen species and D2 receptor stimulation. 2005;102(34):12218-12223. doi:10.1073/pnas.0502698102
21. Van Oostrom JCH, Maguire RP, Verschuuren-Bemelmans CC, et al. Striatal dopamine D2 receptors, metabolism, and volume in preclinical Huntington disease. 2005;65(6):941-943. doi:10.1212/01.wnl.0000176071.08694.cc
22. Dale RC, Merheb V, Pillai S, et al. Antibodies to surface dopamine-2 receptor in autoimmune movement and psychiatric disorders. *Brain*. 2012;135(Pt 11):3453-3468. doi:10.1093/brain/aws256
23. Groman SM, Jentsch JD. Cognitive control and the dopamine D2-like receptor: a dimensional understanding of addiction. 2012;29(4):295-306. doi:10.1002/da.20897

24. Karimi M, Perlmutter JS. The role of dopamine and dopaminergic pathways in dystonia: insights from neuroimaging. *Tremor Other Hyperkinet Mov (N Y)*. 2015;5:280. doi:10.7916/D8J101XV
25. Reiner A, Albin RL, Anderson KD, D'Amato CJ, Penney JB, Young AB. Differential loss of striatal projection neurons in Huntington disease. 1988;85(15):5733-5737. doi:10.1073/pnas.85.15.5733
26. Deng YP, Albin RL, Penney JB, Young AB, Anderson KD, Reiner A. Differential loss of striatal projection systems in Huntington's disease: a quantitative immunohistochemical study. 2004;27(3):143-164. doi:10.1016/j.jchemneu.2004.02.005
27. Katayama Y, Kawamata T, Tamura T, Hovda DA, Becker DP, Tsubokawa T. Calcium-dependent glutamate release concomitant with massive potassium flux during cerebral ischemia in vivo. *Brain Res*. 1991;558(1):136-140.
28. Kondoh T, Korosue K, Lee SH, Heros RC, Low WC. Evaluation of monoaminergic neurotransmitters in the rat striatum during varied global cerebral ischemia. *Neurosurgery*. 1994;35(2):278-285; discussion 285-286.
29. Bird ED. Chemical pathology of Huntington's disease. *Annu Rev Pharmacol Toxicol*. 1980;20:533-551. doi:10.1146/annurev.pa.20.040180.002533
30. Cronberg T, Lilja G, Rundgren M, Friberg H, Widner H. Long-term neurological outcome after cardiac arrest and therapeutic hypothermia. *Resuscitation*. 2009;80(10):1119-1123. doi:10.1016/j.resuscitation.2009.06.021
31. Andersson A-E, Rosén H, Sunnerhagen KS. Life after cardiac arrest: A very long term follow up. *Resuscitation*. 2015;91:99-103. doi:10.1016/j.resuscitation.2015.01.009
32. Tiainen M, Poutiainen E, Oksanen T, et al. Functional outcome, cognition and quality of life after out-of-hospital cardiac arrest and therapeutic hypothermia: data from a randomized controlled trial. *Scand J Trauma Resusc Emerg Med*. 2015;23:12. doi:10.1186/s13049-014-0084-9
33. Grace AA, Bunney BS. Opposing effects of striatonigral feedback pathways on midbrain dopamine cell activity. *Brain Res*. 1985;333(2):271-284.
34. Celada P, Paladini CA, Tepper JM. GABAergic control of rat substantia nigra dopaminergic neurons: role of globus pallidus and substantia nigra pars reticulata. *Neuroscience*. 1999;89(3):813-825.
35. Lee CR, Abercrombie ED, Tepper JM. Pallidal control of substantia nigra dopaminergic neuron firing pattern and its relation to extracellular neostriatal dopamine levels. *Neuroscience*. 2004;129(2):481-489. doi:10.1016/j.neuroscience.2004.07.034

36. Smith Y, Bolam JP. The output neurones and the dopaminergic neurones of the substantia nigra receive a GABA-Containing input from the globus pallidus in the rat. *Journal of Comparative Neurology*. 1990;296(1):47-64. doi:10.1002/cne.902960105
37. Tepper JM, Lee CR. GABAergic control of substantia nigra dopaminergic neurons. *Prog Brain Res*. 2007;160:189-208. doi:10.1016/S0079-6123(06)60011-3
38. Robinson RG. Neuropsychiatric consequences of stroke. *Annu Rev Med*. 1997;48:217-229. doi:10.1146/annurev.med.48.1.217
39. Hachinski V. Post-stroke depression, not to be underestimated. *Lancet*. 1999;353(9166):1728. doi:10.1016/S0140-6736(99)00139-7
40. Hajnal A, Norgren R. Taste pathways that mediate accumbens dopamine release by sapid sucrose. *Physiol Behav*. 2005;84(3):363-369. doi:10.1016/j.physbeh.2004.12.014
41. Hajnal A, Smith GP, Norgren R. Oral sucrose stimulation increases accumbens dopamine in the rat. *Am J Physiol Regul Integr Comp Physiol*. 2004;286(1):R31-37. doi:10.1152/ajpregu.00282.2003
42. Berridge KC, Ho C-Y, Richard JM, DiFeliceantonio AG. The tempted brain eats: Pleasure and desire circuits in obesity and eating disorders. *Brain Res*. 2010;1350:43-64. doi:10.1016/j.brainres.2010.04.003
43. Felger JC, Miller AH. Cytokine effects on the basal ganglia and dopamine function: the subcortical source of inflammatory malaise. *Front Neuroendocrinol*. 2012;33(3):315-327. doi:10.1016/j.yfrne.2012.09.003
44. Felger JC, Treadway MT. Inflammation Effects on Motivation and Motor Activity: Role of Dopamine. *Neuropsychopharmacology*. 2017;42(1):216-241. doi:10.1038/npp.2016.143
45. Miller AH, Haroon E, Raison CL, Felger JC. Cytokine targets in the brain: impact on neurotransmitters and neurocircuits. *Depress Anxiety*. 2013;30(4):297-306. doi:10.1002/da.22084
46. Janata A, Magnet IAM, Uray T, et al. Regional TNF α mapping in the brain reveals the striatum as a neuroinflammatory target after ventricular fibrillation cardiac arrest in rats. *Resuscitation*. 2014;85(5):694-701. doi:10.1016/j.resuscitation.2014.01.033
47. Pang KCH, Sinha S, Avcu P, et al. Long-lasting suppression of acoustic startle response after mild traumatic brain injury. *J Neurotrauma*. 2015;32(11):801-810. doi:10.1089/neu.2014.3451
48. Braff DL, Light GA, Swerdlow NR. Prepulse inhibition and P50 suppression are both deficient but not correlated in schizophrenia patients. *Biol Psychiatry*. 2007;61(10):1204-1207. doi:10.1016/j.biopsych.2006.08.015

49. Geyer MA, Braff DL. Startle habituation and sensorimotor gating in schizophrenia and related animal models. *Schizophr Bull.* 1987;13(4):643-668. doi:10.1093/schbul/13.4.643
50. Swerdlow NR, Paulsen J, Braff DL, Butters N, Geyer MA, Swenson MR. Impaired prepulse inhibition of acoustic and tactile startle response in patients with Huntington's disease. *J Neurol Neurosurg Psychiatry.* 1995;58(2):192-200.
51. Carlson S, Willott JF. Caudal pontine reticular formation of C57BL/6J mice: responses to startle stimuli, inhibition by tones, and plasticity. *J Neurophysiol.* 1998;79(5):2603-2614. doi:10.1152/jn.1998.79.5.2603
52. Lingenhöhl K, Friauf E. Giant neurons in the rat reticular formation: a sensorimotor interface in the elementary acoustic startle circuit? *J Neurosci.* 1994;14(3 Pt 1):1176-1194.
53. Koch M, Schnitzler H-U. The acoustic startle response in rats—circuits mediating evocation, inhibition and potentiation. *Behavioural Brain Research.* 1997;89(1):35-49. doi:10.1016/S0166-4328(97)02296-1
54. Sridharan D, Prashanth PS, Chakravarthy VS. The role of the basal ganglia in exploration in a neural model based on reinforcement learning. *Int J Neural Syst.* 2006;16(2):111-124. doi:10.1142/S0129065706000548
55. O'Keefe J, Nadel L. *The Hippocampus as a Cognitive Map.* Clarendon Press ; Oxford University Press; 1978.
56. Winter B, Juckel G, Viktorov I, et al. Anxious and hyperactive phenotype following brief ischemic episodes in mice. *Biol Psychiatry.* 2005;57(10):1166-1175. doi:10.1016/j.biopsych.2005.02.010
57. Kilic E, Kilic U, Bacigaluppi M, et al. Delayed melatonin administration promotes neuronal survival, neurogenesis and motor recovery, and attenuates hyperactivity and anxiety after mild focal cerebral ischemia in mice. *J Pineal Res.* 2008;45(2):142-148. doi:10.1111/j.1600-079X.2008.00568.x
58. Milot M, Plamondon H. Ischemia-induced hyperactivity: effects of dim versus bright illumination on open-field exploration and habituation following global ischemia in rats. *Behav Brain Res.* 2008;192(2):166-172. doi:10.1016/j.bbr.2008.03.044
59. Milot MR, Plamondon H. Time-dependent effects of global cerebral ischemia on anxiety, locomotion, and habituation in rats. *Behavioural Brain Research.* 2009;200(1):173-180. doi:10.1016/j.bbr.2009.01.009
60. Clauss R, Nel W. Drug induced arousal from the permanent vegetative state. *NeuroRehabilitation.* 2006;21(1):23-28.
61. Clauss RP, Güldenpfennig WM, Nel HW, Sathekge MM, Venkannagari RR. Extraordinary arousal from semi-comatose state on zolpidem. A case report. *S Afr Med J.* 2000;90(1):68-72.

62. Kim C, Kwon BS, Nam KY, Park JW, Lee HJ. Zolpidem-Induced Arousal by Paradoxical GABAergic Stimulation: A Case Report With F-18 Flumazenil Positron Emission Tomography and Single Photon Emission Computed Tomography Study. *Ann Rehabil Med.* 2016;40(1):177-181. doi:10.5535/arm.2016.40.1.177
63. Davis WA., Linsenmeyer M., Wagner AK. Donepezil and Zolpidem Associated Emergence from Disordered Consciousness after Cardiac Arrest: Modulating cholinergic and GABAergic Striato-pallidal-thalamic Circuitry. . *In Review, Neurocase.* Published online 2019.
64. Pinto SM., Kandt JA., Ferimer S, Wagner AK. Donepezil and Zolpidem Associated Emergence from Disordered Consciousness after Cardiac Arrest: Implications involving Striatal Circuitry and Dopamine Modulation. *Am J PhysMed & Rehabil.* 2017; 96(3): Supplement 1. A46.
65. Desmarais, LA., Milleville KB., Wagner AK. Zolpidem Treatment of Post-Operative Venous Congestion associated Brain Injury. *In Review, AJPMR.* Published online 2020.
66. Arruda WO, Silva MS, Bertholdo DB, Munhoz RP, Teive HAG. Zolpidem in movement disorders after cardiac arrest. *Parkinsonism & Related Disorders.* 2017;37:114-115. doi:10.1016/j.parkreldis.2017.01.007
67. Bomalaski MN, Claflin ES, Townsend W, Peterson MD. Zolpidem for the Treatment of Neurologic Disorders. *JAMA Neurology.* 2017;74(9):1130. doi:10.1001/jamaneurol.2017.1133
68. Schiff ND. Recovery of consciousness after brain injury: a mesocircuit hypothesis. *Trends in Neurosciences.* 2010;33(1):1-9. doi:10.1016/j.tins.2009.11.002
69. Goetz T, Arslan A, Wisden W, Wulff P. GABA(A) receptors: structure and function in the basal ganglia. *Prog Brain Res.* 2007;160:21-41. doi:10.1016/S0079-6123(06)60003-4
70. Shoykhet M, Simons DJ, Alexander H, Hosler C, Kochanek PM, Clark RSB. Thalamocortical Dysfunction and Thalamic Injury after Asphyxial Cardiac Arrest in Developing Rats. *J Neurosci.* 2012;32(14):4972-4981. doi:10.1523/JNEUROSCI.5597-11.2012
71. Aravamuthan BR, Shoykhet M. Long-term increase in coherence between the basal ganglia and motor cortex after asphyxial cardiac arrest and resuscitation in developing rats. *Pediatr Res.* 2015;78(4):371-379. doi:10.1038/pr.2015.114
72. Thibaut A, Schiff N, Giacino J, Laureys S, Gosseries O. Therapeutic interventions in patients with prolonged disorders of consciousness. *The Lancet Neurology.* 2019;18(6):600-614. doi:10.1016/s1474-4422(19)30031-6
73. Brefel-Courbon C, Payoux P, Ory F, et al. Clinical and imaging evidence of zolpidem effect in hypoxic encephalopathy. *Annals of Neurology.* 2007;62(1):102-105. doi:10.1002/ana.21110

74. Thonnard M, Gosseries O, Demertzi A, et al. Effect of zolpidem in chronic disorders of consciousness: a prospective open-label study. *Funct Neurol*. Published online January 11, 2014:1-6.
75. Whyte J, Myers R. Incidence of clinically significant responses to zolpidem among patients with disorders of consciousness: a preliminary placebo controlled trial. *Am J Phys Med Rehabil*. 2009;88(5):410-418. doi:10.1097/PHM.0b013e3181a0e3a0
76. Whyte J, Rajan R, Rosenbaum A, et al. Zolpidem and restoration of consciousness. *Am J Phys Med Rehabil*. 2014;93(2):101-113. doi:10.1097/PHM.0000000000000069
77. Carrillo P, Takasu A, Safar P, et al. Prolonged severe hemorrhagic shock and resuscitation in rats does not cause subtle brain damage. *J Trauma*. 1998;45(2):239-248; discussion 248-249.
78. Katz L, Ebmeyer U, Safar P, Radovsky A, Neumar R. Outcome model of asphyxial cardiac arrest in rats. *J Cereb Blood Flow Metab*. 1995;15(6):1032-1039. doi:10.1038/jcbfm.1995.129
79. Janata A, Drabek T, Magnet IAM, et al. Extracorporeal versus conventional cardiopulmonary resuscitation after ventricular fibrillation cardiac arrest in rats: a feasibility trial. *Crit Care Med*. 2013;41(9):e211-222. doi:10.1097/CCM.0b013e318287f51e
80. Harun R, Hare KM, Brough ME, et al. Fast-scan cyclic voltammetry demonstrates that L-DOPA produces dose-dependent regionally selective, bimodal effects on striatal dopamine kinetics in vivo. *J Neurochem*. Published online November 27, 2015. doi:10.1111/jnc.13444
81. Paxinos G, Watson C. *The Rat Brain in Stereotaxic Coordinates*. 6th ed. Elsevier; 2007.
82. Wightman RM, Zimmerman JB. Control of dopamine extracellular concentration in rat striatum by impulse flow and uptake. *Brain research Brain research reviews*. 1990;15(2):135-144.
83. Lam Y-W, Sherman SM. Functional Organization of the Thalamic Input to the Thalamic Reticular Nucleus. *J Neurosci*. 2011;31(18):6791-6799. doi:10.1523/JNEUROSCI.3073-10.2011
84. Yeo SS, Chang PH, Jang SH. The ascending reticular activating system from pontine reticular formation to the thalamus in the human brain. *Front Hum Neurosci*. 2013;7:416. doi:10.3389/fnhum.2013.00416
85. Bariselli S, Fobbs WC, Creed MC, Kravitz AV. A competitive model for striatal action selection. *Brain Res*. 2019;1713:70-79. doi:10.1016/j.brainres.2018.10.009
86. Tanimura A, Pancani T, Lim SAO, et al. Striatal cholinergic interneurons and Parkinson's disease. *Eur J Neurosci*. 2018;47(10):1148-1158. doi:10.1111/ejn.13638

87. Nair AG, Castro LRV, El Khoury M, et al. The high efficacy of muscarinic M4 receptor in D1 medium spiny neurons reverses striatal hyperdopaminergia. *Neuropharmacology*. 2019;146:74-83. doi:10.1016/j.neuropharm.2018.11.029
88. Calabresi P, Picconi B, Tozzi A, Ghiglieri V, Di Filippo M. Direct and indirect pathways of basal ganglia: a critical reappraisal. *Nat Neurosci*. 2014;17(8):1022-1030. doi:10.1038/nn.3743
89. Haber SN. Corticostriatal circuitry. *Dialogues Clin Neurosci*. 2016;18(1):7-21.
90. Schiff ND, Posner JB. Another "Awakenings." 2007;62(1):5-7. doi:10.1002/ana.21158
91. Sieghart W, Sperk G. Subunit composition, distribution and function of GABA(A) receptor subtypes. *Curr Top Med Chem*. 2002;2(8):795-816. doi:10.2174/1568026023393507
92. Chen L, Savio Chan C, Yung W-H. Electrophysiological and behavioral effects of zolpidem in rat globus pallidus. *Experimental Neurology*. 2004;186(2):212-220. doi:10.1016/j.expneurol.2003.11.003
93. Chen L, Xie J-X, Fung K-S, Yung W-H. Zolpidem modulates GABA(A) receptor function in subthalamic nucleus. *Neurosci Res*. 2007;58(1):77-85. doi:10.1016/j.neures.2007.02.002
94. Benhamou L, Bronfeld M, Bar-Gad I, Cohen D. Globus Pallidus External Segment Neuron Classification in Freely Moving Rats: A Comparison to Primates. *PLoS One*. 2012;7(9). doi:10.1371/journal.pone.0045421
95. Hattori T, Fibiger HC, McGeer PL. Demonstration of a pallido-nigral projection innervating dopaminergic neurons. *J Comp Neurol*. 1975;162(4):487-504. doi:10.1002/cne.901620406
96. Chergui K, Charléty PJ, Akaoka H, et al. Tonic activation of NMDA receptors causes spontaneous burst discharge of rat midbrain dopamine neurons in vivo. *Eur J Neurosci*. 1993;5(2):137-144. doi:10.1111/j.1460-9568.1993.tb00479.x
97. Chergui K, Akaoka H, Charléty PJ, Saunier CF, Buda M, Chouvet G. Subthalamic nucleus modulates burst firing of nigral dopamine neurones via NMDA receptors. *Neuroreport*. 1994;5(10):1185-1188. doi:10.1097/00001756-199406020-00006
98. Connelly ST, Shepard PD. Competitive NMDA receptor antagonists differentially affect dopamine cell firing pattern. *Synapse*. 1997;25(3):234-242. doi:10.1002/(SICI)1098-2396(199703)25:3<234::AID-SYN2>3.0.CO;2-C
99. Saji M, Cohen M, Blau AD, Wessel TC, Volpe BT. Transient forebrain ischemia induces delayed injury in the substantia nigra reticulata: degeneration of GABA neurons, compensatory expression of GAD mRNA. *Brain Res*. 1994;643(1-2):234-244. doi:10.1016/0006-8993(94)90030-2

100. van den Brule JMD, van der Hoeven JG, Hoedemaekers CWE. Cerebral Perfusion and Cerebral Autoregulation after Cardiac Arrest. *Biomed Res Int.* 2018;2018. doi:10.1155/2018/4143636
101. Iordanova B, Li L, Clark RSB, Manole MD. Alterations in Cerebral Blood Flow after Resuscitation from Cardiac Arrest. *Front Pediatr.* 2017;5:174. doi:10.3389/fped.2017.00174
102. Park H-P, Nimmagadda A, DeFazio RA, Busto R, Prado R, Ginsberg MD. Albumin therapy augments the effect of thrombolysis on local vascular dynamics in a rat model of arteriolar thrombosis: a two-photon laser-scanning microscopy study. *Stroke.* 2008;39(5):1556-1562. doi:10.1161/STROKEAHA.107.502195
103. Györfly BA, Kun J, Török G, et al. Local apoptotic-like mechanisms underlie complement-mediated synaptic pruning. *Proc Natl Acad Sci USA.* 2018;115(24):6303-6308. doi:10.1073/pnas.1722613115
104. Calabresi P, Centonze D, Bernardi G. Cellular factors controlling neuronal vulnerability in the brain: a lesson from the striatum. *Neurology.* 2000;55(9):1249-1255. doi:10.1212/wnl.55.9.1249
105. Maletic V, Robinson M, Oakes T, Iyengar S, Ball SG, Russell J. Neurobiology of depression: an integrated view of key findings. *Int J Clin Pract.* 2007;61(12):2030-2040. doi:10.1111/j.1742-1241.2007.01602.x
106. Kapur S, John Mann J. Role of the dopaminergic system in depression. *Biological Psychiatry.* 1992;32(1):1-17. doi:10.1016/0006-3223(92)90137-O
107. Dranovsky A, Hen R. Hippocampal neurogenesis: regulation by stress and antidepressants. *Biol Psychiatry.* 2006;59(12):1136-1143. doi:10.1016/j.biopsych.2006.03.082
108. Manji HK, Drevets WC, Charney DS. The cellular neurobiology of depression. *Nat Med.* 2001;7(5):541-547. doi:10.1038/87865
109. Ressler KJ, Nemeroff CB. Role of serotonergic and noradrenergic systems in the pathophysiology of depression and anxiety disorders. *Depress Anxiety.* 2000;12 Suppl 1:2-19. doi:10.1002/1520-6394(2000)12:1+<2::AID-DA2>3.0.CO;2-4
110. Müller MB, Holsboer F. Mice with mutations in the HPA-system as models for symptoms of depression. *Biol Psychiatry.* 2006;59(12):1104-1115. doi:10.1016/j.biopsych.2006.02.008
111. Mayberg HS. Modulating dysfunctional limbic-cortical circuits in depression: towards development of brain-based algorithms for diagnosis and optimised treatment. *Br Med Bull.* 2003;65:193-207. doi:10.1093/bmb/65.1.193
112. Bodien YG, Chatelle C, Edlow BL. Functional Networks in Disorders of Consciousness. *Semin Neurol.* 2017;37(5):485-502. doi:10.1055/s-0037-1607310

113. Dantzer R, Kelley KW. Twenty years of research on cytokine-induced sickness behavior. *Brain Behav Immun.* 2007;21(2):153-160. doi:10.1016/j.bbi.2006.09.006
114. Brooks N, Campsie L, Symington C, Beattie A, McKinlay W. The five year outcome of severe blunt head injury: a relative's view. *J Neurol Neurosurg Psychiatry.* 1986;49(7):764-770. doi:10.1136/jnnp.49.7.764
115. Hibbard MR, Uysal S, Kepler K, Bogdany J, Silver J. Axis I psychopathology in individuals with traumatic brain injury. *J Head Trauma Rehabil.* 1998;13(4):24-39. doi:10.1097/00001199-199808000-00003
116. Felger JC, Hernandez CR, Miller AH. Levodopa reverses cytokine-induced reductions in striatal dopamine release. *Int J Neuropsychopharmacol.* 2015;18(4). doi:10.1093/ijnp/pyu084
117. Janata A, Drabek T, Magnet IAM, et al. Extracorporeal versus conventional cardiopulmonary resuscitation after ventricular fibrillation cardiac arrest in rats: a feasibility trial. *Crit Care Med.* 2013;41(9):e211-222. doi:10.1097/CCM.0b013e318287f51e
118. Lee Y, López DE, Meloni EG, Davis M. A Primary Acoustic Startle Pathway: Obligatory Role of Cochlear Root Neurons and the Nucleus Reticularis Pontis Caudalis. *J Neurosci.* 1996;16(11):3775-3789. doi:10.1523/JNEUROSCI.16-11-03775.1996
119. Hormigo S, López DE, Cardoso A, Zapata G, Sepúlveda J, Castellano O. Direct and indirect nigrothalamic projections to the nucleus reticularis pontis caudalis mediate in the motor execution of the acoustic startle reflex. *Brain Struct Funct.* 2018;223(6):2733-2751. doi:10.1007/s00429-018-1654-9
120. Freund B, Kaplan PW. Myoclonus After Cardiac Arrest: Where Do We Go From Here? *Epilepsy Curr.* 2017;17(5):265-272. doi:10.5698/1535-7597.17.5.265
121. Elmer J, Torres C, Aufderheide TP, et al. Association of early withdrawal of life-sustaining therapy for perceived neurological prognosis with mortality after cardiac arrest. *Resuscitation.* 2016;102:127-135. doi:10.1016/j.resuscitation.2016.01.016
122. Wijdicks EF, Parisi JE, Sharbrough FW. Prognostic value of myoclonus status in comatose survivors of cardiac arrest. *Ann Neurol.* 1994;35(2):239-243. doi:10.1002/ana.410350219
123. Kanthasamy AG, Yun RJ, Nguyen B, Truong DD. Effect of riluzole on the neurological and neuropathological changes in an animal model of cardiac arrest-induced movement disorder. *J Pharmacol Exp Ther.* 1999;288(3):1340-1348.
124. Kanthasamy AG, Nguyen BQ, Truong DD. Animal model of posthypoxic myoclonus: II. Neurochemical, pathologic, and pharmacologic characterization. *Movement Disorders.* 2000;15(S1):31-38. doi:10.1002/mds.870150707
125. Winblad B. Piracetam: A Review of Pharmacological Properties and Clinical Uses. *CNS Drug Rev.* 2005;11(2):169-182. doi:10.1111/j.1527-3458.2005.tb00268.x

126. Doya K. Complementary roles of basal ganglia and cerebellum in learning and motor control. *Curr Opin Neurobiol.* 2000;10(6):732-739. doi:10.1016/s0959-4388(00)00153-7
127. Hoshi E, Tremblay L, Féger J, Carras PL, Strick PL. The cerebellum communicates with the basal ganglia. *Nat Neurosci.* 2005;8(11):1491-1493. doi:10.1038/nn1544
128. Bostan AC, Strick PL. The Cerebellum and Basal Ganglia are Interconnected. *Neuropsychol Rev.* 2010;20(3):261-270. doi:10.1007/s11065-010-9143-9
129. Sieghart W, Sperk G. Subunit composition, distribution and function of GABA(A) receptor subtypes. *Curr Top Med Chem.* 2002;2(8):795-816. doi:10.2174/1568026023393507
130. Grace AA, Bunney BS. Paradoxical GABA excitation of nigral dopaminergic cells: indirect mediation through reticulata inhibitory neurons. *Eur J Pharmacol.* 1979;59(3-4):211-218. doi:10.1016/0014-2999(79)90283-8
131. Martin GE, Haubrich DR. Striatal dopamine release and contraversive rotation elicited by intranigally applied muscimol. *Nature.* 1978;275(5677):230-231. doi:10.1038/275230a0
132. Santiago M, Westerink BH. The role of GABA receptors in the control of nigrostriatal dopaminergic neurons: dual-probe microdialysis study in awake rats. *Eur J Pharmacol.* 1992;219(2):175-181. doi:10.1016/0014-2999(92)90294-e
133. Martin LJ. The Striatal Mosaic in Primates: Striosomes and Matrix Are Differentially Enriched in Ionotropic Glutamate Receptor Subunits. :11.
134. Salinas AG, Davis MI, Lovinger DM, Mateo Y. Dopamine dynamics and cocaine sensitivity differ between striosome and matrix compartments of the striatum. *Neuropharmacology.* 2016;108:275-283. doi:10.1016/j.neuropharm.2016.03.049
135. Ztaou S, Amalric M. Contribution of cholinergic interneurons to striatal pathophysiology in Parkinson's disease. *Neurochemistry International.* 2019;126:1-10. doi:10.1016/j.neuint.2019.02.019
136. Jeon J, Dencker D, Wörtwein G, et al. A Subpopulation of Neuronal M4 Muscarinic Acetylcholine Receptors Plays a Critical Role in Modulating Dopamine-Dependent Behaviors. *J Neurosci.* 2010;30(6):2396-2405. doi:10.1523/JNEUROSCI.3843-09.2010
137. Aoki S, Liu AW, Zucca A, Zucca S, Wickens JR. Role of Striatal Cholinergic Interneurons in Set-Shifting in the Rat. *J Neurosci.* 2015;35(25):9424-9431. doi:10.1523/JNEUROSCI.0490-15.2015
138. Pisani A, Bernardi G, Ding J, Surmeier DJ. Re-emergence of striatal cholinergic interneurons in movement disorders. *Trends in Neurosciences.* 2007;30(10):545-553. doi:10.1016/j.tins.2007.07.008
139. Kuroiwa M, Hamada M, Hieda E, et al. Muscarinic receptors acting at pre- and post-synaptic sites differentially regulate dopamine/DARPP-32 signaling in striatonigral and

striatopallidal neurons. *Neuropharmacology*. 2012;63(7):1248-1257.
doi:10.1016/j.neuropharm.2012.07.046

140. Foster DJ, Gentry PR, Lizardi-Ortiz JE, et al. M5 receptor activation produces opposing physiological outcomes in dopamine neurons depending on the receptor's location. *J Neurosci*. 2014;34(9):3253-3262. doi:10.1523/JNEUROSCI.4896-13.2014
141. Thibault D, Albert PR, Pineyro G, Trudeau L-É. Neurotensin triggers dopamine D2 receptor desensitization through a protein kinase C and beta-arrestin1-dependent mechanism. *J Biol Chem*. 2011;286(11):9174-9184. doi:10.1074/jbc.M110.166454